Nebraska Transportation Center

MID-AMERICA TRANSPORTATION CENTER

NDOR Nebraska Department of Roads

Report MPM-04

Final Report
26-1107-0106-001

Moisture Sensitivity of Hot Mix Asphalt (HMA) Mixtures in Nebraska – Phase II

Yong-Rak Kim, Ph.D.
Associate Professor
Department of Civil Engineering
University of Nebraska-Lincoln

Hoki Ban, Ph.D.
Postdoctoral Research Associate
Ingryd Pinto, M.S.
Graduate Research Assistant

2009

Nebraska Transportation Center
262 WHIT
2200 Vine Street
Lincoln, NE 68583-0851
(402) 472-1975

"This report was funded in part through grant[s] from the Federal Highway Administration [and Federal Transit Administration], U.S. Department of Transportation. The views and opinions of the authors [or agency] expressed herein do not necessarily state or reflect those of the U. S. Department of Transportation."

Moisture Sensitivity of Hot Mix Asphalt (HMA) Mixtures in Nebraska – Phase II

Yong-Rak Kim, Ph.D.
Associate Professor
Department of Civil, Architectural, and Environmental Engineering
University of Nebraska–Lincoln

Hoki Ban, Ph.D.
Postdoctoral Research Associate
Department of Civil, Architectural, and Environmental Engineering
University of Nebraska–Lincoln

Ingryd Pinto, M.S.
Graduate Research Assistant
Department of Civil, Architectural, and Environmental Engineering
University of Nebraska–Lincoln

A Report on Research Sponsored by

Nebraska Department of Roads

November 2009

Technical Report Documentation Page

1. Report No MPM-04	2. Government Accession No.	3. Recipient's Catalog No.	
4. Title and Subtitle Moisture Sensitivity of Hot Mix Asphalt (HMA) Mixtures in Nebraska – Phase II		5. Report Date November 13, 2009	
		6. Performing Organization Code	
7. Author/s Ingryd Pinto, Yongrak Kim, and Hoki Ban		8. Performing Organization Report No. MPM-04	
9. Performing Organization Name and Address University of Nebraska-Lincoln W351 NH, PO Box 880531 Lincoln, NE 68588		10. Work Unit No. (TRAIS)	
		11. Contract or Grant No. 26-1107-0106-001	
12. Sponsoring Organization Name and Address Nebraska Department of Roads 1500 Hwy. 2 Lincoln, NE 68502		13. Type of Report and Period Covered	
		14. Sponsoring Agency Code MATC RiP # 13601	
15. Supplementary Notes			
16. Abstract As a consequential effort to the previous NDOR research project (P564) on moisture damage, this report presents outcomes from this project incorporated with the previous project. Performance changes and fundamental material characteristics associated with moisture damage due to various anti-stripping additives in asphalt mixtures are studied through various experimental approaches and a numerical simulation. Three additives (i.e., one reference additive, hydrated lime, and two alternative additives: fly ash and cement) are investigated by adding them into two types of mixes (*SP2* for low-traffic-volume roadways and *SP5* for high-traffic-volume roadways) where two different asphalt binders (PG 64-22 for the *SP2* mix and PG 70-28 for the *SP5*) are used. Two asphalt concrete mixture scale performance tests, the AASHTO T-283 and the APA under water, and two local-scale mixture constituent tests, the boiling water test (ASTM D 3625) and the pull-off test, are conducted to characterize the effects of binder-specific anti-stripping additives on the binder-aggregate bonding potential in mixtures. The pull-off tensile strength tests are then numerically modeled through the finite element technique incorporated with the cohesive zone modeling approach to seek more fundamental scientific insights into the effect of each anti-stripping additive on the overall moisture damage resistance. Results from laboratory tests and numerical simulations indicate that the *SP5* mixtures, where high-quality aggregates and polymer-modified binder are used, are fairly self-resistant to moisture damage without treating any anti-stripping additive and do not show any visible sensitivity among additives, whereas the effects of additives and their sensitivity are significant in the *SP2* mixes that use the unmodified binder PG 64-22 and low-quality aggregates. With the limited amount of test data, hydrated lime seems to perform slightly better than other additives, particularly with longer moisture-conditioning time. Fly ash contributes to reducing moisture damage by improving binder-aggregate interfacial properties, which are validated from the integrated experimental-computational evaluation.			
17. Key Words Moisture Damage, Asphalt, Hydrated Lime, Fly Ash, Pavement Performance	18. Distribution Statement		
19. Security Classification (of this report) Unclassified	20. Security Classification (of this page) Unclassified	21. No. of Pages 88	22. Price

Form DOT F 1700.7 (8-72) Reproduction of form and completed page is authorized

Table of Contents

Acknowledgments vi
Disclaimer vii
Abstract viii
Chapter 1 Introduction 1
1.1 Research Objectives 3
1.2 Research Scope 4
1.3 Organization of the Report 4
Chapter 2 Background 6
2.1 Moisture-Damage Mechanisms in Asphalt Pavements 9
2.2 Effects of anti-stripping additives 12
2.3 Test methods to asses moisture susceptibility 19
Chapter 3 Research Methodology 23
3.1 Materials Selection 23
3.1.1 Aggregates 24
3.1.2 Asphalt binder 25
3.1.3 Hydrated lime 26
3.1.4 Fly ash 28
3.1.5 Portland cement 28
3.2 Mix Design Method 29
3.3 Performance Evaluation of Asphalt Concrete Mixes 34
3.3.1 AASHTO T-283 35
3.3.2 Asphalt pavement analyzer (APA) testing under water 37
3.4 Local-scale Testing to Characterize Bonding Potential 39
3.4.1 Boiling water test (ASTM D 3625) 39
3.4.2 Pull-off test using the PATTI 40
3.5 Numerical Modeling of Pull-off Testing 48
3.5.1 Finite element mesh 48
3.5.2 Modeling methodology: coupled moisture diffusion–mechanical loading 49
Chapter 4 Results and Discussion 55
4.1 Mix Design Results 55
4.2 Performance Testing Resulting of Asphalt Concrete Mixes 56
4.2.1 AASHTO T-283 testing results 56
4.2.2 APA testing results 60
4.3 Local-scale Test Results 63
4.3.1 Boiling water test results 64
4.3.2 Pull-off test results 67
4.4 Numerical Model Simulation Results 72
4.4.1 Materials and their properties (model inputs) 72
4.4.2 Model simulation and results 77
Chapter 5 Summary and Conclusions 81
5.1 Conclusions 81
5.2 Recommended Further Studies 83
5.3 NDOR Implementation Plan 83
References 85

List of Figures

Figure 2.1 Moisture damage in the United States (Hicks 1991) 7
Figure 2.2 Moisture damage in the United States (Aschenbrener 2002) 8
Figure 2.3 Illustration of moisture-damage mechanisms (Kim and Lutif 2006) 9
Figure 2.4 Effectiveness rating of additives (Hicks 1991) 13
Figure 2.5 Use of fly ash in the United States 16
Figure 3.1 SP5 mixes designed for this study 30
Figure 3.2 Aggregates gradation curve of the mix NF (reference mix) 31
Figure 3.3. Preparing mixtures HL, FA, and CM 33
Figure 3.4 Schematic view of AASHTO T-283 testing 37
Figure 3.5 Typical AASHTO T-283 testing result 37
Figure 3.6 Asphalt Pavement Analyzer (APA) 38
Figure 3.7 Asphalt mixture submitted to boiling water test 40
Figure 3.8 Pneumatic Adhesion Tensile Testing Instrument (PATTI) 41
Figure 3.9 Cross-section view of piston attached to pull-stub 42
Figure 3.10 Procedure used to control binder thickness 43
Figure 3.11 Sample preparation procedure 45
Figure 3.12 A typical set of test results from the pull-off PATTI test 46
Figure 3.13 Finite Element Mesh 49
Figure 3.14 Moisture diffusion profiles after a 24-hr immersion 50
Figure 3.15 Bilinear cohesive zone model and its damage criterion 52
Figure 3.16 Vertical stress contour plots 54
Figure 4.1 Typical AASHTO T-283 test results (Kim and Lutif 2006) 57
Figure 4.2 AASHTO T-283 test results 58
Figure 4.3 TSR results of each mixture 58
Figure 4.4 Combined AASHTO T-283 results from SP2 and SP5 mixtures 60
Figure 4.5 APA test results (SP5 mixtures) 61
Figure 4.6 Combined APA test results from SP2 and SP5 mixtures 63
Figure 4.7 Pictures taken from reference cases (NF) 64
Figure 4.8 Digital image analysis with reference mixture (NF) 66
Figure 4.9 Digital image analysis results from the boiling water test 67
Figure 4.10 Pull-off test results from mixtures with binder PG 64-22 68
Figure 4.11 Pull-off test results from mixtures with binder PG 70-28 69
Figure 4.12 Type of failure 71
Figure 4.13 Relationship between two scale test results 72
Figure 4.14 Strength ratio vs. degree of saturation 76
Figure 4.15 Moisture diffusion profiles at the soaking time 77
Figure 4.16 Model simulations vs. test results (NF Samples) 78
Figure 4.17 Comparison of bond strengths 79
Figure 4.18 Comparison of degradation characteristic curves 80

List of Tables

Table 2.1 Fly ash produced and utilized in the United States and in Nebraska.....17
Table 2.2 Moisture sensitivity tests on compacted mixtures (Solaimanian et al. 2003).....21
Table 2.3 Moisture sensitivity tests on loose mixtures (Solaimanian et al. 2003).....21
Table 3.1 Fundamental properties of aggregates.....24
Table 3.2 Asphalt binder properties of PG 70-28.....25
Table 3.3 Asphalt binder properties of PG 64-22.....26
Table 3.4 Physical properties of hydrated lime.....27
Table 3.5 Chemical properties of hydrated lime.....27
Table 3.6 Chemical properties of class C fly ash.....28
Table 3.7 Chemical properties of cement used in this study.....29
Table 3.8 Amount of each additive in the 10,000-gram aggregate blend.....32
Table 3.9 Required volumetric parameters and aggregate properties for SP5 mix.....34
Table 4.1 Volumetric mix properties and aggregate properties.....56
Table 4.2 Boiling water test results (visual analysis).....65
Table 4.3 PO-TSR values.....69
Table 4.4 Moisture diffusion coefficients employed for the modeling.....73
Table 4.5 Mechanical material properties of aggregate and binder.....74
Table 4.6 CZ properties of each sample at dry condition.....75

Acknowledgments

The authors thank the Nebraska Department of Roads (NDOR) for the financial support needed to complete this study. In particular, the authors thank NDOR Technical Advisory Committee (TAC), Moe Jamshidi, Bob Rea, Mick Syslo, Amy Starr, Brandon Varilek, Matt Beran, Lieska Halsey, and Jodi Gibson for their technical support and invaluable discussions/comments. The authors also wish to thank Dr. Codrin Daranga and Professor Hussain Bahia at the University of Wisconsin-Madison sharing invaluable information on the PATTI testing. Special thanks to Larry Koves and Jody Gregory in the NDOR for their help for the APA testing

Disclaimer

This report was funded in part through grant[s] from the Federal Highway Administration [and Federal Transit Administration], U.S. Department of Transportation. The views and opinions of the authors [or agency] expressed herein do not necessarily state or reflect those of the U. S. Department of Transportation.

Abstract

As a consequential effort to the previous NDOR research project (P564) on moisture damage, this report presents outcomes from this project incorporated with the previous project. Performance changes and fundamental material characteristics associated with moisture damage due to various anti-stripping additives in asphalt mixtures are studied through various experimental approaches and a numerical simulation. Three additives (i.e., one reference additive, hydrated lime, and two alternative additives: fly ash and cement) are investigated by adding them into two types of mixes (*SP2* for low-traffic-volume roadways and *SP5* for high-traffic-volume roadways) where two different asphalt binders (PG 64-22 for the *SP2* mix and PG 70-28 for the *SP5*) are used. Two asphalt concrete mixture scale performance tests, the AASHTO T-283 and the APA under water, and two local-scale mixture constituent tests, the boiling water test (ASTM D 3625) and the pull-off test, are conducted to characterize the effects of binder-specific anti-stripping additives on the binder-aggregate bonding potential in mixtures. The pull-off tensile strength tests are then numerically modeled through the finite element technique incorporated with the cohesive zone modeling approach to seek more fundamental scientific insights into the effect of each anti-stripping additive on the overall moisture damage resistance. Results from laboratory tests and numerical simulations indicate that the *SP5* mixtures, where high-quality aggregates and polymer-modified binder are used, are fairly self-resistant to moisture damage without treating any anti-stripping additive and do not show any visible sensitivity among additives, whereas the effects of additives and their sensitivity are significant in the *SP2* mixes that use the unmodified binder PG 64-22 and low-quality aggregates. With the limited amount of test data, hydrated lime seems to perform slightly better than other additives, particularly with longer moisture-conditioning time. Fly ash contributes to reducing moisture damage by improving binder-aggregate interfacial properties, which are validated from the integrated experimental-computational evaluation.

Chapter 1 Introduction

Prior to this project, the University of Nebraska-Lincoln (UNL) research team had completed a research project (P564) on the subject of moisture sensitivity of asphalt mixtures (the so-called *SP2* mix) generally used for low-volume local pavements in Nebraska. The project investigated effects of hydrated lime with two different forms (dry and slurry) and mineral filler as a moisture-damage-resisting agent by performing various traditional asphalt concrete tests (i.e., asphalt pavement analyzer (APA) testing under water, Hamburg wheel-tracking testing, and AASHTO T-283 tensile strength ratio evaluation with different freeze-thaw cycles) and a few fundamental property-related tests (i.e., surface energy measurements of binder/mastic and aggregates, linear viscoelastic stiffness measurements of binder/mastic through dynamic shear rheometer (DSR), and fracture-damage testing of binder/mastic) to estimate material properties of mix components for further analyses of material-dependent moisture damage mechanisms.

Experimental data demonstrated clear effects of hydrated lime as an active material due to its synergistic damage-mitigating mechanisms: a stiffening effect that results in better resistance to moisture attack and improved bonding characteristics between mastic and aggregates, which significantly reduces stripping problems in the presence of moisture. It was also true that additional filler in the mix would be helpful to mitigate the initial level of moisture damage due to its stiffening effect on asphalt binder.

Successful accomplishments of the previous research project (P564) resulted in consequential research needs with extended scopes, including 1) evaluation of moisture sensitivity of different Superpave mixes in Nebraska, and 2) use of potential moisture-damage-resisting agents as alternatives to hydrated lime. Based on kickoff meetings with members of the Nebraska Department of Roads (NDOR) Technical Advisory Committee (TAC), a Superpave

SP5 was selected as a target mix type for this project due to its significance as a primary mix type mostly for high-volume interstate highway pavements and its distinct mixture characteristics from the mix *SP2*. The *SP5* mix consists of better-quality (e.g., more crushed) aggregates and polymer-modified asphalt binder PG 70-28, while the *SP2* mix is usually produced with less-angular aggregates and unmodified asphalt binder PG 64-22. Therefore, there is a need to evaluate the impact of aggregate surface modification through crushing and binder modification with polymers on moisture-induced damage characteristics, since adhesive bonding potential between aggregate and asphalt will be critically controlled by physical-chemical reactions of mix components (i.e., aggregate and asphalt) with anti-stripping agents treated in the mix. Alternative additives such as fly ash and cement were also investigated as potential (supplemental) anti-stripping agents, because they are more convenient to access than hydrated lime, which must be transported from other states, resulting in additional costs. In particular, fly ash is a waste material with a large amount of daily production. Its application in asphalt mixtures can potentially bring benefits to the environment and reduce the amount of disposed material in landfill sites.

A similar testing plan developed for project P564 was employed for this project. Laboratory tests of asphalt concrete mixtures are composed of 1) volumetric mixture design of various *SP5* mixes treated with different anti-stripping agents (i.e., hydrated lime, fly ash, and cement), and 2) fabrication of compacted asphalt concrete samples and mechanical testing of the asphalt concrete samples using traditional performance evaluation techniques such as AASHTO T-283 and APA under water. Furthermore, the bonding between aggregate and binder at a local-scale level was investigated following the boiling water test (ASTM D 3625) and the pull-off test using a Pneumatic Adhesion Tensile Testing Instrument (PATTI) procedure so that measured

characteristics of each mix component can be related to performance testing results of asphalt concrete samples. The PATTI has gained attention in the scientific community because it contributes to a better understanding of the local-scale debonding characteristics between aggregate and binder in the presence of water, which leads to a better evaluation of material-specific moisture susceptibility. The pull-off test conducted at different levels of moisture conditioning with the different applications of anti-stripping additive was simulated by a sequentially coupled moisture diffusion–mechanical loading finite element (FE) analysis. The cohesive zone modeling (CZM) was incorporated in the FE analysis to simulate adhesive fracture at the binder-aggregate interface with different applications of anti-stripping additive. Results from the model simulation can scientifically identify how each anti-stripping additive contributes to the mixtures' moisture-damage resistance.

Research outcomes from this study are incorporated with findings from the previous project (P564) to produce more detailed and comprehensive information and to ultimately improve Superpave specifications currently used in Nebraska.

1.1 Research Objectives

The primary goal of this research is to provide testing-analysis results and consequent findings that can help demonstrate the effects of various anti-stripping additives (i.e., hydrated lime, cement, and fly ash) on moisture-damage resistance and their physical-mechanical mechanisms with two frequently used asphalt binders (PG 64-22 and 70-28) in Nebraska pavements. Research outcomes from this study are then incorporated with research findings from the previous NDOR project (P564) to draw more comprehensive and general conclusions based on results from diverse mixes (*SP2* and *SP5*).

1.2 Research Scope

To accomplish the objectives, this research has been divided into four phases. Phase one consists of a literature review, material selection, and volumetric mixture design of target mixtures. The second phase is defined as the global-scale laboratory effort, which includes the fabrication of asphalt concrete specimens and their mechanical tests to estimate the tensile strength (AASHTO T-283) and the rutting performance (APA under water). The focus of the third phase was the local-scale level, which evaluates the stripping resistance resulting from the treatment of anti-stripping additives at aggregate-binder interface. The boiling water test (ASTM D 3625) and the pull-off testing with the PATTI were performed. Test results between two scales (global and local) were compared and related. The fourth phase of this research, as mentioned, was the numerical modeling of the pull-off testing to provide more scientific insight into the material-dependent characteristics of anti-stripping additives on moisture-damage resistance of mixtures.

1.3 Organization of the Report

This report is composed of five chapters. Following this introduction (Chapter 1), Chapter 2 presents background information associated with moisture-damage mechanisms and related testing-analysis methods, including recent advancements. Chapter 3 presents detailed descriptions of material selection and research methodology employed for this study. Chapter 4 shows laboratory test results, such as volumetric mix design results of all mixes, bulk performance testing results from AASHTO T-283 and APA testing, and local-scale debonding characteristics of mixture constituents through the boiling water test and the PATTI. Chapter 4 also presents an evaluation of the effectiveness of anti-stripping agents on moisture damage in asphalt mixtures through numerical simulation of the PATTI testing. Finally, Chapter 5 provides

a summary of findings and conclusions of this study. Recommended future research and implementation plans for the Nebraska Department of Roads (NDOR) are also presented in the chapter.

Chapter 2 Background

Moisture damage is a major problem in U.S. asphalt pavements, and shows itself in various forms with multiple mechanisms, such as adhesion failure between asphalt and aggregate; moisture-induced cohesion failure within the asphalt binder; cohesion failures within the aggregate; emulsification of the asphalt; and freezing of entrapped water. Among those, the reduction of adhesion between asphalt and aggregates in the presence of water and the deterioration of asphalt due to cohesive failure within the asphalt binder itself have been known as the two primary driving mechanisms of moisture damage since the 1920s (Solaimanian et al. 2003). In 1991, the National Cooperative Highway Research Program (NCHRP) conducted a survey to evaluate the impacts of moisture damage in U.S. pavements. As illustrated in figure 2.1, 70% of states presented premature rutting, raveling and wear in their pavements due to moisture damage (Hicks 1991).

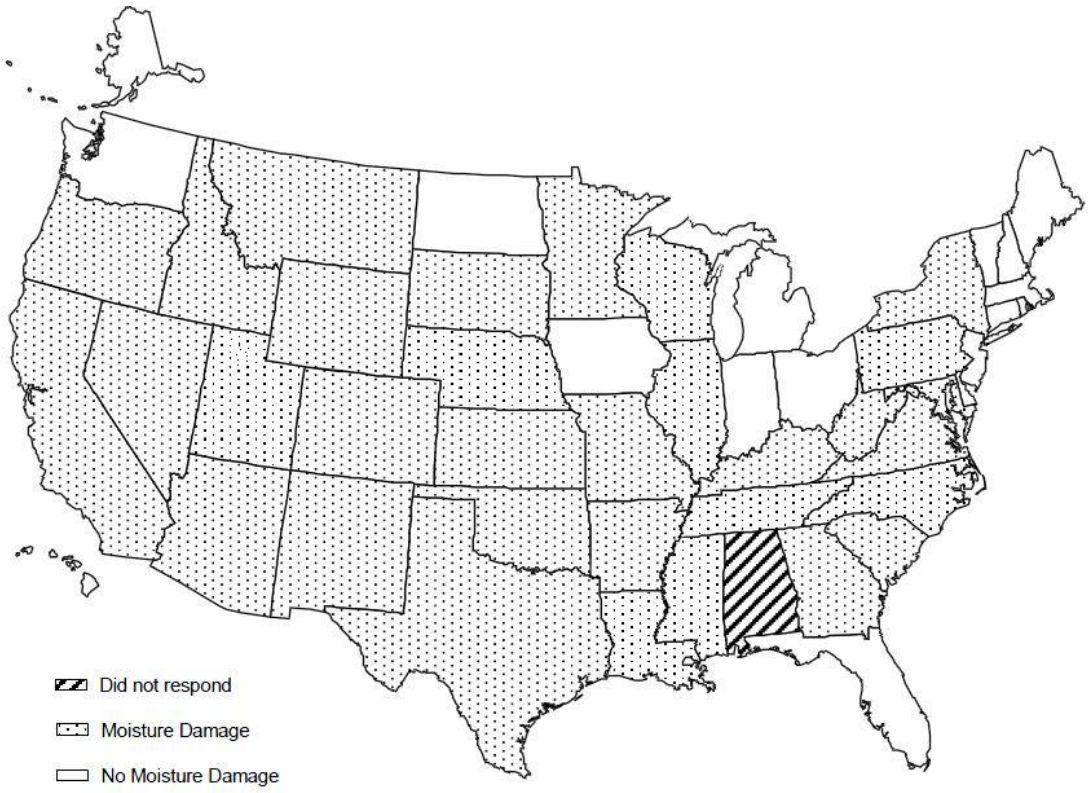

Figure 2.1 Moisture damage in the United States (Hicks 1991)

Later, Aschenbrener (2002) conducted a survey on moisture damage of hot-mix asphalt pavements in the United States and found that a total of 44 states have experienced severe moisture damage in their pavements. To reduce moisture damage, 82%t of the nation's state highway agencies require some sort of anti-strip treatment. Of those agencies that treat, 56% use liquids, 15% use liquid or lime, and 29% treat with lime only, as illustrated in figure 2.2.

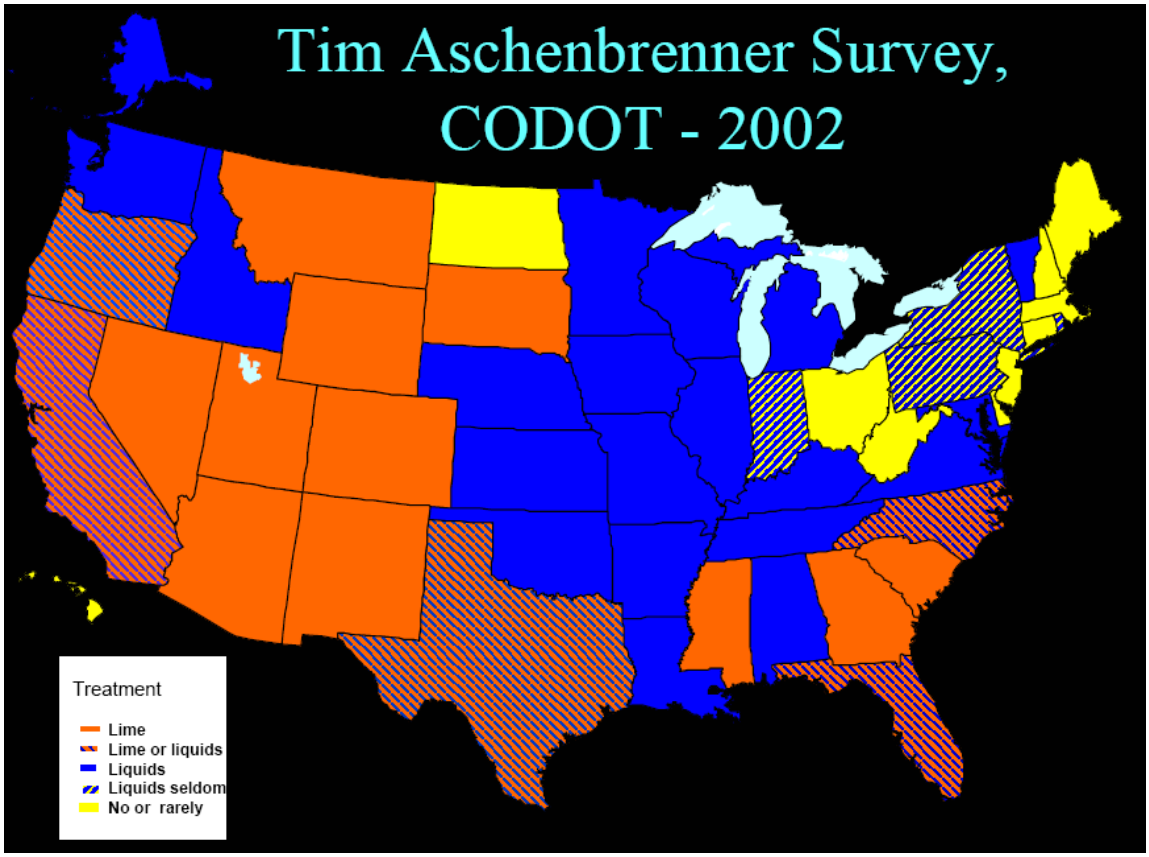

Figure 2.2 Moisture damage in the United States (Aschenbrener 2002)

Due to the great number of U.S. pavements under significant moisture damage, attempts have been made to identify the moisture-damage mechanisms and to develop test procedures that could estimate the moisture susceptibility of asphalt mixtures. Furthermore, many different types of additives have been applied to the asphalt mixtures to minimize moisture-related damage. Hydrated lime is the one additive that has shown its unique effects on moisture-damage mitigation. Therefore, many state highway agencies, including NDOR, employ and/or require the use of hydrated lime in HMA pavements. Recently, the use of alternative additives, such as fly ash, has driven significant attention to the asphalt materials/pavement community. Fly ash is much more economical and convenient to access than hydrated lime in certain states, such as Nebraska, where a large amount of fly ash is produced daily and requires landfills for disposal

and other costly operations. Its application in asphalt mixtures can potentially bring benefits to the environment and reduce the amount of disposed material.

2.1 Moisture-Damage Mechanisms in Asphalt Pavements

Moisture damage is a primary mode of distress in hot-mix asphalt (HMA). Infiltration of moisture into the asphalt mixture can cause stripping, resulting in weakening of the asphalt-aggregate bond and subsequent dislocation of the aggregate, leading to pothole formation (Kringos et al. 2008). As illustrated in figure 2.3 (Kim and Lutif 2006), moisture typically reduces stiffness of the binder and/or mastic through moisture diffusion, and degrades the adhesive bonding between the binder/mastic and aggregate particles. Therefore, a loss of HMA internal strength results in premature distresses such as rutting, raveling, and fatigue cracking. Moisture-damage mechanisms are complex, and attempts have been made to simplify them by categorizing them. Still, identification of the fracture mechanisms of asphalt-aggregate systems in the presence of water is difficult, and a synergistic interaction of mechanisms often remains the best explanation of the moisture-damage process.

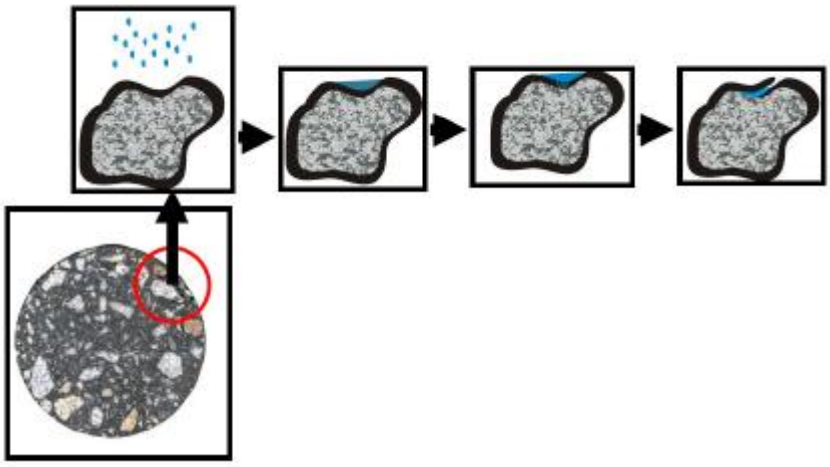

Figure 2.3 Illustration of moisture-damage mechanisms (Kim and Lutif 2006)

The performance of asphalt pavements is related to cohesive and adhesive bonding within the asphalt-aggregate system. The loss of cohesion (strength) and stiffness of the asphalt film, and the failure of the adhesive bond between aggregate and asphalt in conjunction with the degradation or fracture of the aggregate were identified as the main mechanisms of moisture damage in asphalt pavements (Terrel and Al-Swailmi 1994; Kanitpong and Bahia 2003).

A promising approach to assessing moisture-damage potential is to identify fundamental material properties that affect and control moisture damage, and then develop reasonable and efficient testing methods to determine better materials (including anti-stripping agents) and design considerations for resisting moisture-associated damage.

Kim et al. (2004) evaluated the negative effects of moisture damage on material properties of asphalt mixtures. They successfully used the dynamic mechanical analysis (DMA) technique to evaluate fundamental property characteristics of asphalt binders and mastics by measuring fundamental viscoelastic properties. Cylindrical DMA specimens were fabricated using SHRP-classified binders and Ottawa sand to perform various dynamic tests in both wet and dry conditions and to determine the viscoelastic stiffness of specimens. Testing results clearly demonstrated a significant reduction in the dynamic shear moduli (stiffness) due to the presence of moisture, which might be due to moisture penetration into the mastic or into the mastic-sand interface.

The mechanisms that govern adhesive failure in the asphalt-aggregate system are even more complex, since the adhesion between two distinct phases is related to mechanical and chemical reactions, molecular attractions, and interfacial energy theory, as mentioned by Mohamed (1993). Several attempts have been made to explain the loss of adhesive bonding between the asphalt film and the aggregate in the presence of water. The differences in

physicochemical properties at the surface of the combined materials used in HMA mixtures are attributed as important factors regarding the adhesive failure of the asphalt-aggregate system. Surface free energy of asphalt binders and aggregates is one such important physicochemical property. In 2003, Cheng et al. proposed an adhesion failure model to analyze the adhesive fracture in the asphalt-aggregate interface in the presence of water. They hypothesized that adhesive failure was clearly related to the surface energy of the asphalt-aggregate system. They calculated the work of adhesion between the asphalt and the aggregates based on the surface free energy theory, and then using the adhesion failure model, they identified the moisture-damage potential of asphalt mixtures. To verify the validity of the model, a comparison was made between the results from the model and the results from repeated-load permanent deformation tests on asphalt mixtures either in dry or wet conditions. Test results validated the adhesion failure model and also showed that, for the same asphalt, granite mixtures are more vulnerable to moisture damage than limestone mixtures.

In addition to the two primary driving mechanisms (i.e., cohesive failure of asphalt films and adhesive failure of asphalt-aggregate interfaces), some other phenomena, such as displacement, detachment, and pore pressure buildup, are some of the effects of a moisture-attacked pavement that lead to adhesive and cohesive failure of the asphalt pavements (Lytton et al. 2005). Displacement involves debonding of the asphalt film from the aggregate surface through a break in the asphalt film. The break in the asphalt film is due to several reasons, including incomplete coating of the aggregate surface, traffic load, and freeze-thaw (F-T) cycles that stress the pavement. Detachment results from the penetration of water between the aggregate-binder systems without actually breaking the asphalt film. Pore pressure buildup

occurs when the pavement is in a saturated condition due to moisture attack. With the buildup of pore pressure, the microcracks start to grow and eventually rupture the asphalt film.

In order to reduce the stripping, anti-stripping agents have typically been used in asphalt mixtures. Numerous studies indicate that anti-stripping additives can positively affect the binder-aggregate bonding characteristics and overall mixture performance by reducing mixtures' moisture susceptibility (Kennedy and Ping 1991).

2.2 Effects of Anti-Stripping Additives

Evaluation of many different types of additives/modifiers and their appropriate application methods to maximize moisture-damage resistance of HMA mixtures has been an important issue, resulting in many studies. One well-known anti-stripping additive is hydrated lime. Hydrated lime provides better adhesive compatibility between aggregate and asphalt mastic. Thus, the use of hydrated lime may increase bonding characteristics between aggregate and asphalt. Furthermore, it has also been demonstrated that hydrated lime significantly changes rheological properties of asphalt systems. Many experimental results have shown that adding hydrated lime to asphalt mixtures significantly improves moisture-damage resistance, especially when subjected to the wetting-drying treatment (Fwa and Ong 1994; McCann and Sebaaly 2003; and many more). Based on these facts, 1.0% hydrated lime by weight of total dry aggregates in a mix is currently required for Superpave mixes used in Nebraska pavements.

According to a study by Hicks (1991), along with amines and Portland cement, hydrated lime was generally more effective than polymers in preventing moisture damage. Furthermore, as shown in figure 2.4, the effectiveness of lime is quite consistent (small standard deviation) compared to other additives, such as the amines. The effectiveness of the amines ranges widely, which indicates highly dependent effectiveness on the asphalt-aggregate combinations. Sufficient

literature strongly supports the use of hydrated lime to control moisture sensitivity of asphalt mixtures and also to induce other benefits due to lime addition, such as stiffening the asphalt binder and HMA, improvements in the resistance to fracture growth at low temperatures, and favorable oxidation kinetics and interactions with products of oxidation to reduce deleterious effects by aging (Aschenbrener 1995; Little and Epps 2001; McCann and Sebaaly 2003).

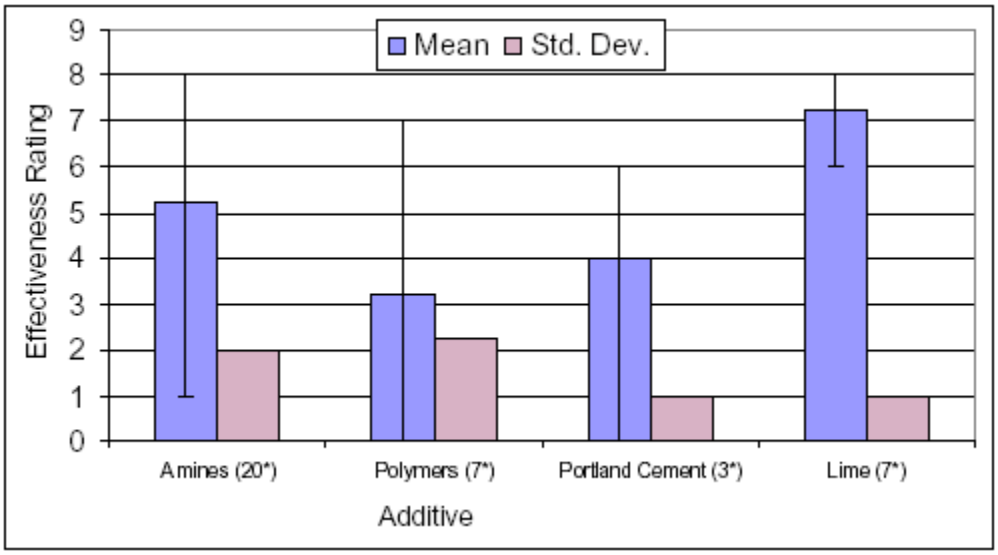

Figure 2.4 Effectiveness rating of additives (Hicks 1991)

Ping (1993) conducted a laboratory investigation to monitor the effectiveness of lime to protect HMA mixtures from moisture damage. He used lime in slurry form with 1.0% of lime by weight of total aggregates, and conducted AASHTO T-283 testing to obtain tensile strengths from either wet or dry samples. The hydrated lime showed a positive effect by enhancing the tensile strength ratio of mixtures.

In 2005, Huang et al. investigated the impact of lime addition on the moisture resistance of HMA by directly adding lime to the binder (or mastic) prior to mixture preparation. They used

two mineralogically different aggregates: granite with silica and limestone with a high concentration of calcium. With two chemically different aggregate surfaces, the authors were expecting different reactions with polar components of the asphalt, resulting in different moisture-resistant behavior. Based on the indirect tensile strength results, they found that lime treatment of the asphalt prior to mixing produced a stronger mixture.

McCann and Sebaaly (2003) performed another seminal study on this subject. They evaluated the mechanical properties of lime-treated mixtures before and after multiple cycles of freeze-thaw. They also evaluated the effectiveness of lime treatment by varying the method of lime addition: dry lime into moistened aggregates and lime slurry into dry aggregates, with either a 48-hour marination or no marination process. McCann and Sebaaly (2003) measured resilient modulus, tensile strength, and simple shear strain of each mixture. Based on testing results and statistical analyses, they presented the following findings: 1) the addition of lime reduced the moisture-related rutting potential; 2) the method of lime addition did not significantly affect moisture sensitivity of the mixtures; and 3) the resilient modulus showed to be the best indicator to evaluate the mixture's moisture susceptibility, specifically for specimens that show minimal differences between unconditioned and conditioned tensile strength.

More recently, as presented earlier, the PI and his UNL research team performed a research project (P564) on the subject of moisture sensitivity of asphalt mixtures (*SP2* mix) to investigate the effects of hydrated lime with two different forms (dry and slurry). Various traditional asphalt concrete tests (i.e., asphalt pavement analyzer [APA] testing under water, Hamburg wheel-tracking testing, and AASHTO T-283 tensile strength ratio evaluation with different freeze-thaw cycles) and several fundamental property-related tests (i.e., surface energy measurements of binder/mastic and aggregates, linear viscoelastic stiffness measurements of

binder/mastic through dynamic shear rheometer [DSR], and fracture-damage testing of binder/mastic) were conducted in the project. Testing data and analyses clearly demonstrated that hydrated lime contributed to moisture-damage resistance due to the synergistic effects of mastic stiffening and advanced bonding characteristics at mastic-aggregate interfaces. However, to maximize benefits from lime addition, evenly distributed and well-dispersed lime treatment onto aggregate surfaces was necessary. Specifically, treatments of lime slurry need more care. More detailed test results and related discussion can be found elsewhere (Kim and Lutif 2006; Kim et al. 2008).

Since this research evaluates fly ash and Portland cement as potential alternative anti-stripping agents that could replace hydrated lime, literature searches on those materials related to pavement performance and moisture-damage resistance have been attempted; however, few studies have been found.

A survey conducted by the American Coal Ash Association (ACAA) provides information about production and application of fly ash from 170 power plants in the United States. In 2007, approximately 72 million tons of fly ash were produced in the United States and only 32 million tons (44.4% of total) were consumed. The remaining material has been deposited in landfill sites. Figure 2.5 presents a chart illustrating the main uses of fly ash. As is well known and presented in the figure, the primary use of fly ash is cement concrete production as a mineral admixture. The use of fly ash in asphalt mixtures is included in the group described as “other” because of its small percentage of the total usage.

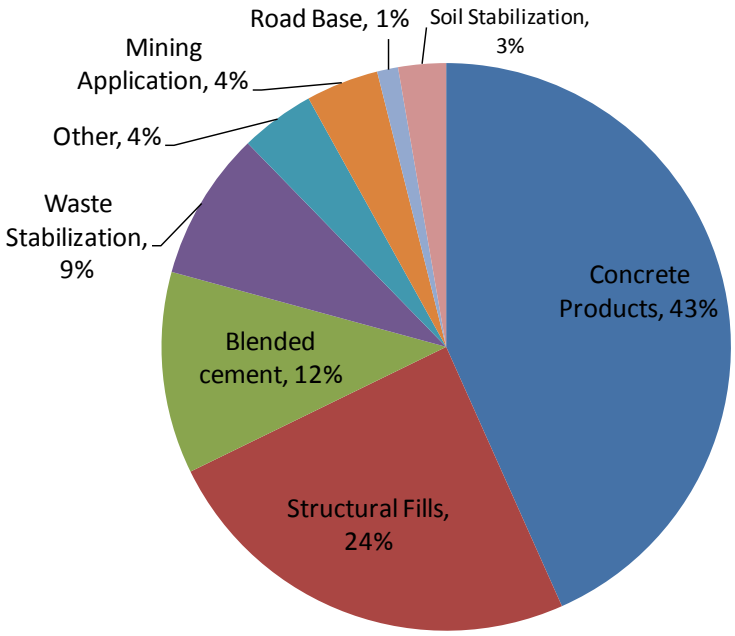

Figure 2.5 Use of fly ash in the United States

There are five utilities with coal-fired power plants in Nebraska: the Nebraska Public Power District (NPPD), with Gerald Gentleman station and Sheldon station; the Omaha Public Power District (OPPD), with North Omaha and Nebraska City power plants; the Hastings Utilities; the Fremont Utilities; and the Grand Island Utilities. Table 2.1 presents the amount of fly ash produced and utilized in the United States and in the state of Nebraska, respectively. For the state of Nebraska, two major power plants (NPPD and OPPD) data were obtained and are presented in the table. As shown, a significant amount of fly ash has been disposed of in landfill sites.

Table 2.1 Fly ash produced and utilized in the United States and in Nebraska

Source	Fly Ash		
	Produced (tons)	Utilized (tons)	Utilized (%)
American Coal Ash Association - USA	71,700,000	31,626,037	44%
NPPD and OPPD - Nebraska	410,381	300,329	73%

The cost of disposing the unused fly ash varies from $12 to $15 per ton; sometimes it can reach $34 per ton. Considering the amount of abandoned fly ash in 2007 from the NPPD and the OPPD, a value of $1,650,780 was spent in the disposal process, not to mention the environmental issues that this by-product can cause. This situation has driven highway engineers and researchers to investigate the use of fly ash for various engineering purposes, such as the application of fly ash in asphalt pavements.

Fly ash can be used as a cost-effective mineral filler in HMA paving applications. Where available locally, fly ash might cost less than other mineral fillers. Also, due to the lower specific gravity of fly ash, similar performance can be obtained using less material by weight, further reducing the material cost of HMA. Mineral fillers increase the stiffness of the asphalt mortar matrix, improving the rutting resistance of pavements. Mineral fillers also help reduce the amount of asphalt draindown in the mix during construction, which improves durability of the mix by maintaining the amount of asphalt initially used in the mix.

Fly ash normally meets mineral-filler specification requirements for gradation, organic impurities, and plasticity. Also, fly ash is known as hydrophobic (non-water-wettable), reducing

the potential for asphalt stripping; the presence of lime in some fly ashes may also reduce stripping potential.

Several previous studies have shown that the addition of fly ash can improve HMA performance. Rosner et al. (1982) presented that the addition of 3% to 6% of fly ash in asphalt mixtures had comparable results for moisture-damage resistance compared to other anti-stripping additives. The improvement of moisture-damage resistance by adding fly ash to the asphalt mixture was also confirmed by Henning (1974) and Dougan (1991). Henning also reported that fly ash works as a stiffening and void-filling agent for the mixture.

Ali et al. (1996) stated that fly ash added in the amount of 2% of total weight of aggregates as a mineral filler improves not only the stiffness characteristics, but also mixture strength and stripping resistance. However, there was no indication from the study that fly ash would reduce pavement distress and improve field performance.

Portland cement has also been added to aggregates, and has been reported to be generally effective in reducing moisture susceptibility of HMA mixtures; however, contrary to the popularity of hydrated lime, it has not been used widely except in a limited number of states. Recently, a couple of studies on the effectiveness of Portland cement in moisture-damage resistance in asphalt mixtures have been reported.

Oruc et al. (2007) evaluated the addition of Portland cement on emulsified asphalt mixtures by varying the percentage of this additive from 0% to 6% as mineral filler. Resilient modulus of mixtures, before and after soaking in water, was measured and the ratio was used to evaluate moisture-damage performance. Mixtures without the addition of cement failed after six hours of conditioning. However, emulsified asphalt mixtures with cement showed better water resistance and an increase in the resilient modulus.

A study conducted by Hao and Liu (2006) showed the effectiveness of various anti-stripping agents by performing the AASHTO T-283 tests. Mixtures treated with 1% (by total weight of aggregates) of dry lime, lime slurry, Portland cement, and liquid anti-stripping agents were applied in three different aggregate sources: granite, limestone, and schist. The granite mixture showed poor water-stripping performance compared to the other materials. Test results demonstrated that lime slurry treatment performed the best and the Portland cement slightly improved moisture-damage resistance.

2.3 Test Methods to Asses Moisture Susceptibility

A number of testing methods have been developed to predict and evaluate moisture susceptibility of asphalt mixtures. A standard method, "Resistance of Compacted Bituminous Mixture to Moisture-Induced Damage" in AASHTO T-283, has been developed by the National Cooperative Highway Research Program (NCHRP) 4-08 and 10-17 projects and is widely-used to assess moisture susceptibility of asphalt mixtures by simply comparing indirect tensile strength of asphalt concrete samples with and without freeze-thaw (F-T) moisture conditioning. This test procedure is also known as a modified Lottman test procedure since it was developed based on work done by Lottman (1978), and further modified through the work of Tunnicliff and Root (1982).

Investigations in rutting performance associated with moisture damage have also been adopted by conducting two popular testing methods of asphalt concrete samples: the Hamburg wheel-tracking test and the asphalt pavement analyzer (APA) test under water. However, those tests are performed in the laboratory using asphalt concrete samples applied under a fixed load at a fixed temperature, making it impracticable to predict moisture damage of mixtures under traffic loads and different environmental conditions (Epps et al. 2000). Furthermore, the tests

(AASHTO T-283, Hamburg, and APA) are somewhat costly and time-consuming, and are limited in validating detail damage mechanisms of asphalt mixtures due to moisture attack.

Including the aforementioned three popular tests, a number of qualitative and quantitative test methods have been developed to predict and evaluate moisture susceptibility of asphalt mixtures. Qualitative tests are based on subjective evaluation of the stripping potential of hot-mix asphalt (HMA) mixtures, while quantitative tests provide a specific value, such as strength before and after moisture conditioning. Solaimanian et al. (2003) categorized each of the test procedures developed to identify moisture susceptibility of HMA mixtures. Basically, the tests can be divided into two categories: (1) tests on compacted mixtures, and (2) tests on loose mixtures. Tables 2.2 and 2.3 summarize the traditional moisture-sensitivity tests on compacted and loose mixtures, respectively.

Aschenbrener et al. (1995) performed a postmortem study on 20 pavements that had shown significant performance degradation related to moisture damage. For the study, four tests were conducted: traditional AASHTO T-283, ASTM D 3625 (boiling water test), testing with the environmental condition system (ECS), and the Hamburg testing. All mixtures were treated with anti-stripping agents. They observed that instantaneous failures were generally related to the combination of high temperature, high moisture level, and high traffic instead of freezing conditions. The authors tried to reproduce mixtures used in the 20 pavements and then evaluated the reliability of the moisture sensitivity tests based on the known field performance. From AASHTO T-283, the prediction of failure due to moisture was successfully achieved for mixtures that lasted less than two years in the actual field (six out of eight). On the other hand, for pavements with high maintenance, this test could not identify their moisture susceptibility.

From the Hamburg results, they also concluded that test conditions are very severe since four of the seven acceptable sites investigated did not pass the Hamburg failure criteria.

Table 2.2 Moisture sensitivity tests on compacted mixtures (Solaimanian et al. 2003)

Test	ASTM	AASHTO	Other
Moisture vapor susceptibility			California Test 307
			Developed in late 1940s
Immersion–compression	D1075	T165	ASTM STP 252 (Goode, 1959)
Marshal immersion			Stuart 1986
Freeze–thaw pedestal test			Kennedy et al. 1982
Original Lottman indirect tension			NCHRP Report 246 (Lottman, 1982); Transportation Research Record 515 (1974)
Modified Lottman indirect tension	T 283		NCHRP Report 274 (Tunnicliff and Root, 1984), Tex 531-C
Tunnicliff–Root	D 4867		NCHRP Report 274 (Tunnicliff and Root, 1984)
ECS with resilient modulus			SHRP-A-403 (Al-Swailmi and Terrel, 1994)
Hamburg wheel tracking			1993 Tex-242-F
Asphalt pavement analyzer			ECS/SPT NCHRP 9-34 2002-03
Multiple freeze–thaw			

Table 2.3 Moisture sensitivity tests on loose mixtures (Solaimanian et al. 2003)

Test	ASTM	AASHTO	Other
Methylene blue			Technical Bulletin 145, International Slurry Seal Association
Film stripping			(California Test 302)
Static immersion	D1664*	T182	
Dynamic immersion			
Chemical immersion			Standard Method TMH1 (Road Research Laboratory, 1986, England)
Surface reaction			Ford et al. (1974)
Quick bottle			Virginia Highway and Transportation Research Council (Maupin, 1980)
Boiling	D3625		Tex 530-C Kennedy et al. 1984
Rolling bottle			Isacsson and Jorgensen, Sweden, 1987
Net adsorption			SHRP A-341 (Curtis *et al*., 1993)
Surface energy			Thelen 1958, HRB Bulletin 192
			Cheng *et al*., AAPT 2002
Pneumatic pull-off			Youtcheff and Aurilio (1997)

* No longer available as ASTM standard.

Although agencies and researchers have extensively used tests performed in laboratories, it is important to note that these tests have been calibrated and implemented on a local basis (a region within a state). No test has been successfully calibrated and implemented across a wide spectrum of conditions. Testing protocols that are somewhat simpler but more reliable and fundamental need to be developed for advanced estimation and prediction of moisture-related damage.

Recently, fundamental material properties and mechanisms to assess moisture susceptibility of asphalt mixtures have been actively pursued in order to overcome the shortcomings of empirical test methods. Many studies (Birgisson et al. 2003; Kanitpong and Bahia 2003; Airey et al. 2005; Solaimanian et al. 2006; Kassem et al. 2006; Bhasin and Little 2007; Copeland 2007; Kringos and Scarpas 2008; Kringos et al. 2008) proposed new concepts associated with key material properties, such as fracture parameters, surface energy, diffusion coefficients, and adhesion characteristics to better identify and understand moisture-damage characteristics of asphalt mixtures.

Chapter 3 Research Methodology

This chapter describes materials used in this research, which include aggregates, three anti-stripping additives (hydrated lime, fly ash, and Portland cement), and asphalt binder. It also illustrates mix design methods to obtain six Superpave mixes (named NF, HL, FA, CM, HNB, and LS) satisfying NDOR *SP5* mix design specifications. Located at the end of this chapter, is a brief description of laboratory tests performed in this study. Two asphalt concrete performance tests, AASHTO T-283 testing and APA (asphalt pavement analyzer) testing under water, were performed to evaluate macroscopic moisture-related sensitivity of mixes. Two local-scale mixture constituent tests, the boiling water test (ASTM D 3625) and the pull-off test using a PATTI, were performed to characterize the bonding potential between aggregate and binder with different treatments of anti-stripping additives. The pull-off tests conducted at different levels of moisture conditioning with the different applications of anti-stripping agent were then computationally modeled to simulate the sequentially coupled moisture diffusion–mechanical analysis procedure. The finite element method (FEM) incorporated with cohesive zone (CZ) modeling was used for the simulation. Model simulations provide more fundamental scientific insights into the effect of each anti-stripping additive on the overall moisture-damage resistance.

3.1 Materials Selection

To accomplish more realistic simulation of HMA mixtures paved in Nebraska, the most widely used local paving materials (aggregates and asphalt binder) were selected for fabricating laboratory samples. Three anti-stripping additives— hydrated lime, which has been used in Nebraska asphalt pavements as a default anti-stripping agent, and two potential alternative additives, fly ash and Portland cement— were selected and evaluated in this study.

3.1.1 Aggregates

A total of six local aggregates (5/8-in. limestone, 1/4-in. limestone, screenings, 2A, 3ACR, and 47B) were used in this project. These aggregates were selected because they are the most widely used by Nebraska pavement contractors. Table 3.1 illustrates laboratory-measured physical properties, such as bulk specific gravity (G_{sb}) and absorption capacity of each aggregate. In addition, important Superpave aggregate consensus properties, coarse aggregate angularity (CAA), fine aggregate angularity (FAA), and sand equivalency (SE), are also presented in the table. As can be seen, each aggregate demonstrates very different characteristics; therefore, a wide range of aggregate blends meeting target specific gravity and angularity can be obtained via appropriate aggregate mixing. For this study, all mixes designed were targeted to be blended with 45% limestone type (5/8-in. limestone, 1/4-in. limestone, and screening) and 55% from gravel type (2A, 47B, and 3ACR).

Table 3.1 Fundamental properties of aggregates

Aggregates		G_{sb}	Angularity (%)	Absorption Capacity (%)	Sand Equivalency (%)
Coarse aggregates	5/8-inch LS	2.631	100	1.25	N/A
	1/4-inch LS	2.606	100	1.54	N/A
	2A	2.586	26	0.68	N/A
Fine aggregates	Screening	2.552	46.73	3.66	26.0
	47B	2.608	37.3	0.49	98.0
	3ACR	2.576	45.7	1.13	84.0

3.1.2 Asphalt binder

Two asphalt binders were used in this study. To fabricate *SP5* mixes and samples, the Superpave performance-graded polymer-modified binder PG 70-28 was used. For the local-scale tests (i.e., the boiling water test and the PATTI pull-off test), the unmodified binder PG 64-22, which has been used mostly for low-volume local roads in Nebraska, was also used to be compared with test results from PG 70-28. Global-scale (i.e., asphalt concrete mixture scale) test results from this project using the polymer-modified binder 70-28 can be compared to mixture test results from the previous research project (P564), where the unmodified binder PG 64-22 was used. Jebro, Inc., located in Sioux City, Iowa, provided both asphalt binders. Tables 3.2 and 3.3 present fundamental properties of each binder by performing dynamic shear rheometer (DSR) tests and bending beam rheometer (BBR) tests, which have been designated in the Superpave binder specification to identify performance grade and viscoelastic properties of asphalt binder.

Table 3.2 Asphalt binder properties of PG 70-28

Test	Temperature (^{o}C)	Test Result	Required Value
Unaged DSR, G*/sinδ (kPa)	70	1.999	min. 1.00
RTFO, Aged DSR G*/sinδ (kPa)	70	2.879	min. 2.20
PAV - Aged DSR, G*sinδ (kPa)	25	1,448	max. 5,000
PAV - Aged BBR, stiffness (MPa)	-18	168	max. 300
PAV - Aged BBR, m-value	-18	0.324	min. 0.30

Table 3.3 Asphalt binder properties of PG 64-22

Test	Temperature (^{o}C)	Test Result	Required Value
Unaged DSR, G*/sinδ (kPa)	64	1.48	min. 1.00
RTFO, Aged DSR G*/sinδ (kPa)	64	3.499	min. 2.20
PAV - Aged DSR, G*sinδ (kPa)	25	4,576	max. 5,000
PAV - Aged BBR, stiffness (MPa)	-12	203.97	max. 300
PAV - Aged BBR, m-value	-12	0.312	min. 0.30

3.1.3 Hydrated lime

The use of hydrated lime has been recommended in many states, including Nebraska, where HMA pavements are susceptible to moisture-related stripping. Hydrated lime has been known to be a promising potential material to reduce moisture damage of pavements due to its unique physical/chemical/mechanical characteristics. This study used hydrated lime in three different forms—dry lime added in wet aggregates, dry lime added directly into binder prior to mixing with aggregates, and lime slurry (lime/water at a ratio of 0.16:1) mixed with dry aggregates—to investigate the effects of hydrated lime depending on its application method. Hydrated lime was obtained from Mississippi Lime Company, located in Sainte Genevieve, Missouri. Tables 3.4 and 3.5 illustrate the basic physical and chemical properties of hydrated lime used for this study.

Table 3.4 Physical properties of hydrated lime

Physical Properties	
Specific Gravity	2.343
Dry Brightness, G.E.	92.0
Median Particle Size - Sedigraph	2 microns
pH	12.4
BET Surface Area	22 m^2/g
-100 Mesh (150 μm)	100.0%
-200 Mesh (150 μm)	99.0%
-350 Mesh (150 μm)	94.0%
Apparent Dry Bulk Density - Loose	22lbs./ft^3
Apparent Dry Bulk Density - Packed	35lbs./ft^3

Table 3.5 Chemical properties of hydrated lime

Chemical Properties	
$CA(OH)_2$ - Total	98.00%
$CA(OH)_2$ - Available	96.80%
CO_2	0.50%
H_20	0.70%
$CaSO_4$	0.10%
Sulfur - Equivalent	0.024%
Crystaline Silica	<0.1%
SiO_2	0.50%
Al_20_3	0.20%
Fe_2O_3	0.06%
MgO	0.40%
P_2O_5	0.010%
MnO	0.0025%

3.1.4 Fly ash

Fly ash was estimated in this study as a possible option for a more economical anti-stripping additive. Class C fly ash with specific gravity of 2.650 was added in a dry form to wet aggregates in this study to evaluate if its addition to the asphalt mixture would improve the moisture-damage resistance. Chemical properties of fly ash used in this study are presented in table 3.6.

Table 3.6 Chemical properties of class C fly ash

Chemical Properties	
Al_2O_3 (%)	17.902
SiO_2 (%)	34.852
Fe_2O_3 (%)	5.399
CaO (%)	26.901
MgO (%)	4.936
SO_3 (%)	1.876
P_2O_5 (%)	0.900
TiO_2 (%)	0.979
Na_2O (%)	1.511
K_2O (%)	0.362

3.1.5 Portland cement

Portland cement Type I–II with specific gravity of 3.150 was also used in this research as another anti-stripping additive that can potentially replace (or supplement) hydrated lime. Cement was obtained from Holcim Mfg. in Florence, Colorado. Table 3.7 shows chemical components of cement.

Table 3.7 Chemical properties of cement used in this study

Chemical Properties	
SiO_2 (%)	19.718
Al_2O_3 (%)	4.894
Fe_2O_3 (%)	3.337
CaO (%)	62.185
MgO (%)	1.2264
SO_3 (%)	2.863
Na_2O (%)	0.2035
K_2O (%)	0.8786
TiO_2 (%)	0.1959
P_2O_5 (%)	0.2017
SrO (%)	0.2004
Cr_2O_3 (%)	0.0173
Mn_2O_3 (%)	0.302
ZnO (%)	0.0213
Cl (%)	0.0055
C_3S (%)	57.48
C_2S (%)	13.17
C_3A (%)	7.32
C_4AF (%)	10.16

3.2 Mix Design Method

As mentioned, six *SP5* mixes (NF, HL, FA, CM, HNB, and LS) were designed to conduct HMA performance tests: AASHTO T-283 and APA under water. Each mix was designed with the same blend of aggregates in order to keep constant overall aggregate angularities (both CAA and FAA) and mineralogical characteristics. The variables to differentiate mixes were the type of additives (hydrated lime, fly ash, or cement) and the application method of hydrated lime (dry lime to wet aggregates, dry lime mixed into binder, and

lime slurry applied to dry aggregates). Figure 3.1 illustrates the six mixes, where "***X***" represents the variation of each mixture.

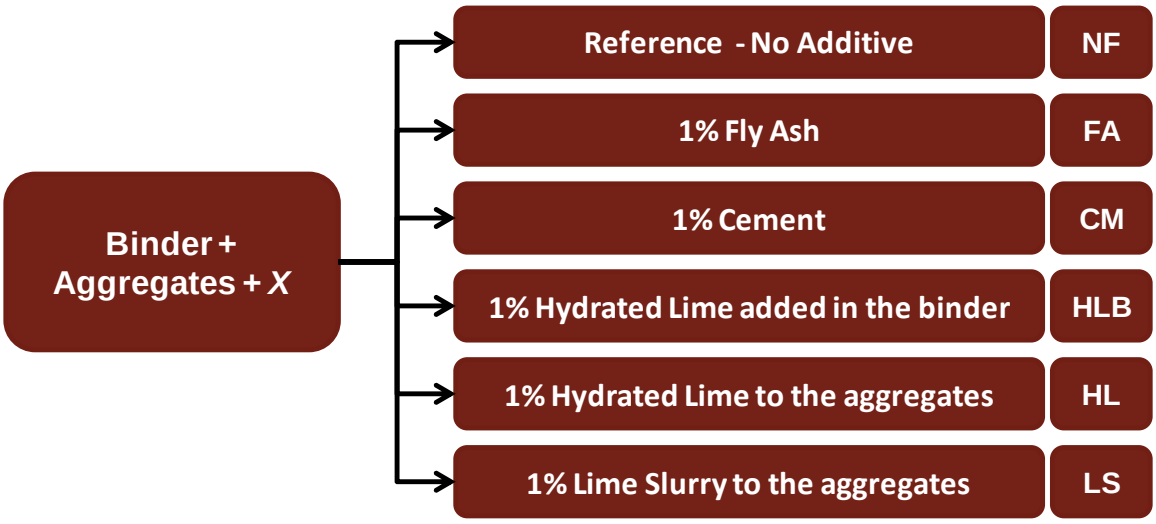

Figure 3.1 *SP5* mixes designed for this study

NF is a reference mix in that no additive is in the mix. Figure 3.2 presents an overall gradation of aggregate blends targeted to form the mix NF. As shown in the figure, the mix is located below restricted zone and contains 3.5% of mineral filler, aggregates passing the No. 200 sieve (0.075 mm mesh size).

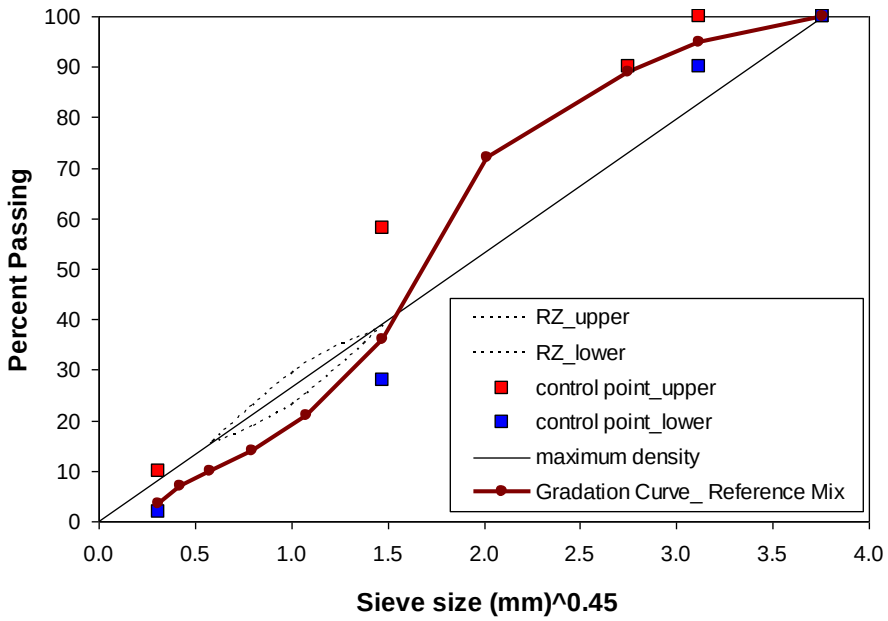

Figure 3.2 Aggregates gradation curve of the mix NF (reference mix)

In order to investigate effects of hydrated lime as an anti-stripping additive, three different mixes, HL, HLB, and LS, were designed. As shown in figure 3.1, an identical amount of hydrated lime (1% by the total weight of dry aggregates) was applied to all three mixes. Comparing mix performance testing results from lime-treated mixes (HL, HLB, or LS) with the mix NF will reveal any benefits obtained from lime addition, and performance variations among HL, HLB, and LS will show effects dependent on treating method of hydrated lime into HMA. Comparing FA and CM mixes to the lime-treated mixes and/or NF, it is possible to evaluate how the addition of two potential alternative anti-stripping additives can affect the moisture susceptibility in the asphalt mixture.

In order to ensure the equivalent volumetric application of each additive in the mixture, the total weight of hydrated lime in the mixtures, HL, HLB, and LS, was converted to its volume with given specific gravity, and the same volume was targeted to estimate the gravimetric

amount of other additives (fly ash and cement). In other words, the other mixtures with different additives were designed such that the volume would be a constant among all the studied mixtures and the weight of each one would vary according to their specific gravity value. Table 3.8 shows the amount of each additive necessary in the 10,000-gram blend of the aggregates.

Table 3.8 Amount of each additive in the 10,000-gram aggregate blend

Additive	Specific Gravity	Volume (g/cm^3)	Weight (g)
Hydrated Lime	2.343	42.68	100.00
Fly Ash	2.650	42.68	113.10
Cement	3.150	42.68	134.44

In order to add the anti-stripping agent to the HL, FA, and CM mixes, 3% of water by total weight of aggregates was added into the blend of aggregates and subsequently mixed so as to wet all of the particles. After mixing the aggregates with water, the anti-stripping agent was added to the wet aggregates and mixed to cover all of the aggregates as much as possible, as shown in figure 3.3. The treated aggregates were then oven-dried for two hours to eliminate all water before the addition of asphalt binder.

(a) Adding Water to Aggregates

(b) Mixing Water in the Aggregates

(c) Adding Additive to the Wet Agrgegates

(d) Mixing Additive with Aggregates

Figure 3.3. Preparing mixtures HL, FA, and CM

For the lime slurry–treated mixture (LS), 1% hydrated lime (by total weight of dry aggregates) was diluted in 6% water, representing a lime/water ratio of 0.16, and then mixed with dry aggregates to produce well-distributed lime-water films on the aggregate surface. Subsequently, the mixture was placed in the oven until dry before mixing with binder. Another lime-treated mixture, the HLB mixture was produced by adding hydrated lime directly to the binder prior to being mixed with the aggregates. The same amount of hydrated lime (1% of total weight of aggregates) was mixed with pure binder. Any influence of the application method of hydrated lime on HMA performance can be evaluated by comparing the mixes (HL, HLB, and LS).

All the mixes designed are *SP5* type, a premium quality mix used mostly for high-traffic volume pavements. The compaction effort used for the *SP5* mix is the one for a traffic volume of approximately 10 to 30 million equivalent single axle loads (ESALs). Table 3.9 summarizes NDOR specification requirements of aggregate properties, volumetric mix design parameters, and laboratory compaction effort for the *SP5* mix. Compaction effort was estimated based on the average value of high air temperature in Omaha, Nebraska: 98ºF (36.67ºC).

Table 3.9 Required volumetric parameters and aggregate properties for *SP5* mix

	NDOR Specification (*SP5* Mix)
Compaction Effort	
N_{ini}: the number of gyration at initial	8
N_{des}: the number of gyration at design	109
N_{max}: the number of gyration at maximum	174
Aggregate Properties	
CAA (%): coarse aggregate angularity	> 95/90
FAA (%): fine aggregate angularity	> 45
SE (%): sand equivalency	> 45
F&E (%): flat and elongated aggregates	< 10
Volumetric Parameters	
$\%V_a$: air voids	4 ± 1
%VMA: voids in mineral aggregates	> 14
%VFA: voids filled with asphalt	65 - 75
$\%P_b$: asphalt content	-
D/B (ratio): dust-binder ratio	0.7 - 1.7

All six mixes, designed in the geomaterials laboratory at the UNL, were submitted to NDOR asphalt/aggregate laboratories for validation of aggregate properties (i.e., Superpave consensus properties of aggregates) and volumetric mix design parameters.

3.3 Performance Evaluation of Asphalt Concrete Mixes

The two most opular performance tests associated with evaluation of HMA moisture damage and susceptibility were conducted in this project: AASHTO T-283 (Resistance of

Compacted Bituminous Mixture to Moisture-Induced Damage) and APA testing of compacted asphalt concrete samples under water.

3.3.1 AASHTO T-283

The evaluation of moisture sensitivity of asphalt concrete samples has been widely accomplished using a standard method, AASHTO T-283. This test procedure was elaborated based on a study by Lottman (1978) and posterior work developed by Tunnicliff and Root (1982). Studies by Witczak et al. (2002), McCann and Sebaaly (2003), and many more have employed this technique for assessing moisture sensitivity of various mixtures and materials due to its simplicity, even if this laboratory evaluation has a relatively low correlation with actual performance in field.

A Superpave gyratory compactor was used to produce testing specimens, 150 mm (4 in) in diameter and 95 ± 5 mm (3.75 ± 0.20 in) height with 7% ± 0.5 air voids. Three subsets of specimens were fabricated and tested, with two subsets subject to partial vacuum saturation, followed by one freeze-thaw (F-T) cycle and six F-T cycles, respectively, prior to being tested. The third subset was tested without the conditioning process.

The unconditioned (no F-T cycle) set of specimens were covered with plastic film and placed inside plastic bags. Then, the specimens were placed in a water bath at 25 ± 0.5ºC (77 ± 1ºF) for two hours to control the specimens' temperature before testing. For the conditioning, each specimen was subjected to partial vacuum saturation for a short period of time to reach its moisture saturation level of around 70% to 80%. Then, the partially saturated specimens were covered with plastic film and placed inside plastic bags. The specimens were then moved into a freezer at a temperature of -18 ± 3ºC (0 ± 5ºF), where they remained for 24 hours. After the freezing cycle, the specimens were moved to a water bath at 60 ± 1ºC (140 ± 2ºF) for 24 hours.

After the freezing-thawing cycle was completed, the specimens were placed in a water bath of 25 ± 0.5ºC (77 ± 1ºF) for two hours before testing.

All specimens were tested to determine their indirect tensile strengths. As demonstrated in figure 3.4, the AASHTO T-283 testing applied a compressive load to a cylindrical specimen through two diametrically opposed rigid platens to induce tensile stress along the diametral vertical axis of the test specimen. A series of splitting tensile strength tests were conducted at a constant strain rate of 2 in. per minute vertically until vertical cracks appeared and the sample fails. A peak compressive load (shown in fig. 3.5) was recorded and used to calculate tensile strength of the sample using the following equation:

$$TS = \frac{2 \cdot P}{\pi \cdot t \cdot D} \tag{3.1}$$

where: TS = tensile strength (psi),

P = peak compressive load (lb),

t = specimen thickness (in), and

D = specimen diameter (in).

Numerical index of resistance of asphalt mixtures to water is expressed as the ratio of the average tensile strength of the unconditioned specimens to the average tensile strength of the conditioned specimens.

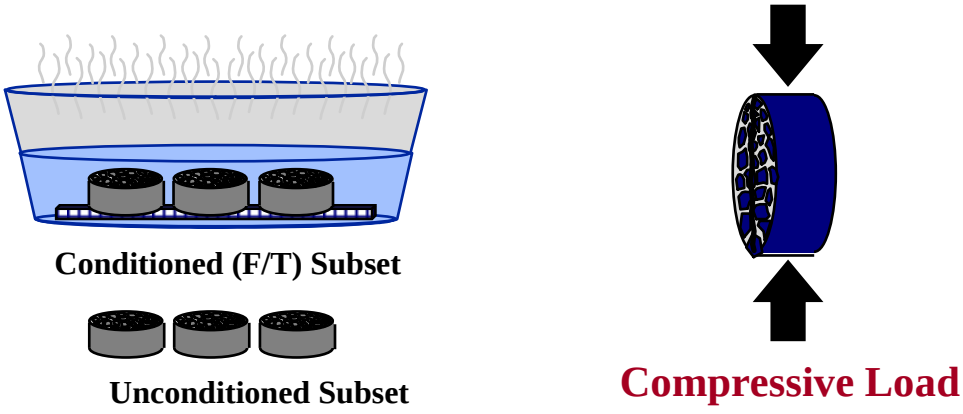

Figure 3.4 Schematic view of AASHTO T-283 testing

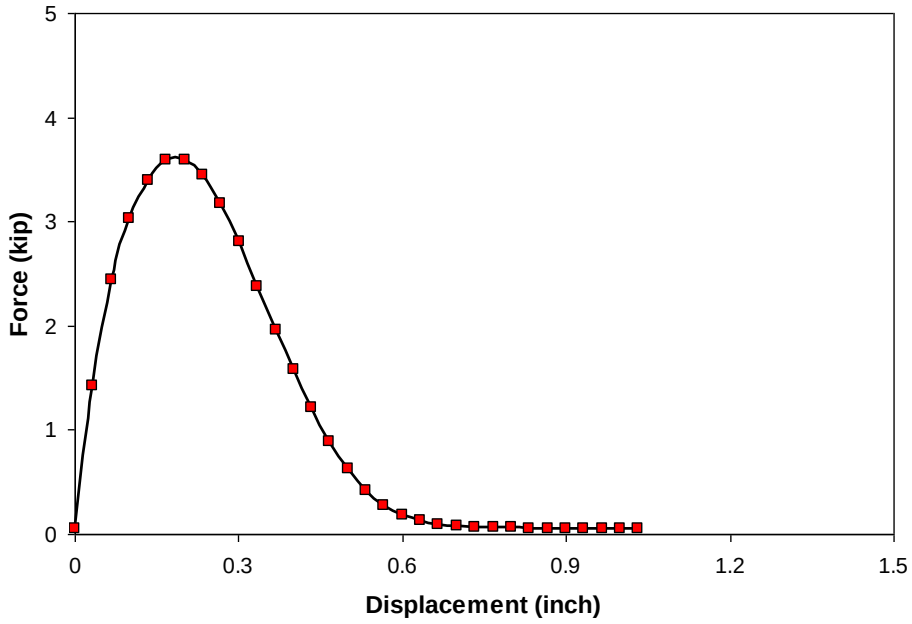

Figure 3.5 Typical AASHTO T-283 testing result

3.3.2 Asphalt pavement analyzer (APA) testing under water

Rutting susceptibility and moisture resistance of asphalt concrete samples can be evaluated using the APA shown in figure 3.6. The APA is an automated, new generation of the Georgia Load Wheel Tester (GLWT) used to evaluate rutting, fatigue, and moisture resistance of

asphalt concrete mixtures. During the APA test, the rutting susceptibility of compacted specimens is tested by applying repetitive linear loads through three pressurized hoses via wheels to simulate trafficking. Even though it has been reported that APA testing results are not very well matched with actual field performance, APA testing is relatively simple to do and produces rutting potential of mixes by simply measuring sample rut depth. To evaluate moisture damage and susceptibility, asphalt concrete samples from each mix are maintained under water at the desired temperature during the test, and submerged deformations are measured with an electronic dial indicator. Due to the simplicity of its testing operation and the fact that the APA testing was performed in the previous research project (P564) that investigated the effects of anti-stripping additives on *SP2* mixes, the APA was employed again in this project. Testing results are presented and discussed in Chapter 4.

(a) APA with Beam and Cylindrical Samples (b) Front View of APA

Figure 3.6 Asphalt Pavement Analyzer (APA)

3.4 Local-Scale Testing to Characterize Bonding Potential

Many studies have demonstrated that moisture typically degrades the adhesive bonding between the binder (or mastic) and aggregate particles. Thus, this research project evaluated the bonding-debonding characteristics at the aggregate-binder interface by performing two local-scale mixture constituent tests: the boiling water test (ASTM D 3625) and the pull-off test using a PATTI device. These tests can characterize directly and/or indirectly the bonding potential between aggregate and binder with the different treatments of anti-stripping additives evaluated in this study. As mentioned earlier and detailed later, the pull-off test results obtained at different levels of moisture conditioning with different treatments of anti-stripping additives are further numerically modeled to produce more fundamental scientific understanding of the moisture-damage-related mechanisms of each additive.

3.4.1 Boiling water test (ASTM D 3625)

The boiling water test is a visual rating of the degree of stripping after boiling the loose HMA mixture for 10 minutes. Approximately 500 ml of water is placed in a 1,000 ml beaker and is heated to boil; 250 g of loose HMA mixture is then heated at a maximum temperature of 100ºC (212°F), but not lower than 80ºC (176°F), and immersed in the boiling water for 10 minutes, as shown in figure 3.7. Once finished, the beaker is removed from the heat source and a paper is used to skim off the bitumen on the water surface to prevent recoating. After cooling it to room temperature, the water is removed, and the mixture is placed onto a white paper towel to be visually analyzed. The criterion of failure is by visual identification of stripped (uncoated) aggregates.

(a) Side View

(b) Top View

Figure 3.7 Asphalt mixture submitted to boiling water test

The boiling water test is extremely simple to perform, but appears to have the potential to evaluate the effect of anti-stripping additives in the mixture to minimize the loss of adhesion between aggregate and asphalt binder. Furthermore, this test has also presented a good correlation between laboratory results and field performance (Parker and Wilson 1986).

3.4.2 Pull-off test using the PATTI

The bond strength between asphalt film and aggregate can be compromised in the presence of water. Thus, understanding this process is important to predict and to prevent the moisture-damage process. Until now, a method to accurately determine mechanical bond strength between these two materials has not been fully established. However, a pull-off test method as specified in the ASTM D 4541, "Pull-off Strength of Coatings Using Portable Adhesion Testers," has been employed by several researchers, such as Kanitpong and Bahia (2003), Copeland (2007), and Cho and Bahia (2007), as a promising approach for characterizing the adhesive bonding potential of asphalt materials. Youtcheff and Aurilio (1997) used this method to evaluate the adhesive bond between aggregate and asphalt film in the presence of water.

The ASTM D 4541 is a methodology originally developed by the painting/adhesive industry to measure the adhesion or pull-off strength of a coating on solid surfaces (e.g., metal, concrete, etc.). This testing method measures the greatest perpendicular force that a solid surface coating can take before the adhesive is detached from the solid surface. The test also allows for the evaluation of the type of failure: adhesive (at the interface between coating and solid surface) or cohesive (within the coating) by inspecting the failure surface after the detachment has occurred.

The equipment used to perform the pull-off test is the PATTI, shown in figure 3.8, which was developed by the National Institute of Standards and Technology (NIST). Figure 3.9 illustrates a cross-section schematic view of the piston attached to a pull-stub.

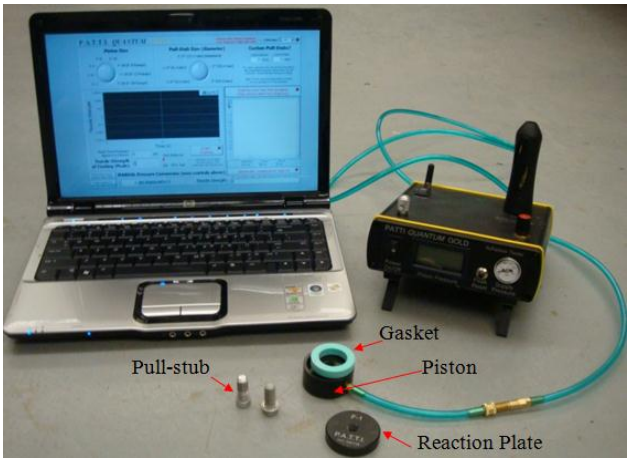

Figure 3.8 Pneumatic Adhesion Tensile Testing Instrument (PATTI)

The PATTI measures the maximum tensile pressure necessary to separate the binder from the aggregate substrate. The thickness of the binder must be controlled precisely and identically in all cases. A similar manner developed by Kanitpong and Bahia (2003), where the binder film

thickness could be controlled by placing two metal supports under the pull-stub, as shown in figure 3.10, was employed in this study. The binder film thickness is the space between the pull-stub and the aggregate surface, which is targeted to be 0.4 mm.

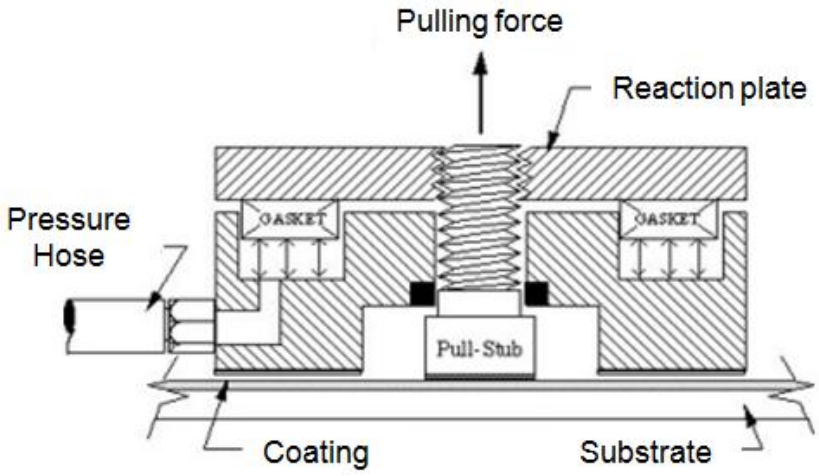

Figure 3.9 Cross-section view of piston attached to pull-stub

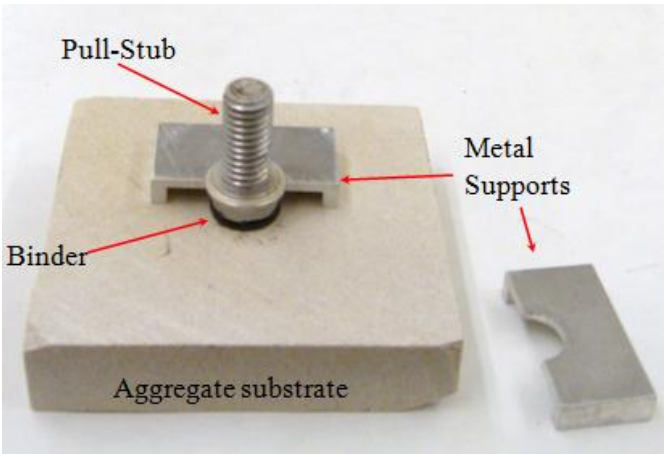

(a) Prepared Sample with Metal Supports

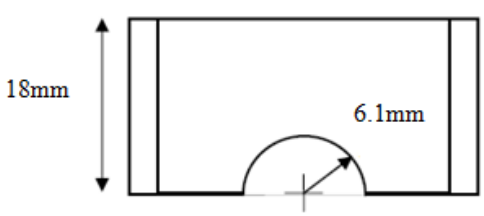

(b) Top View of Support Dimensions

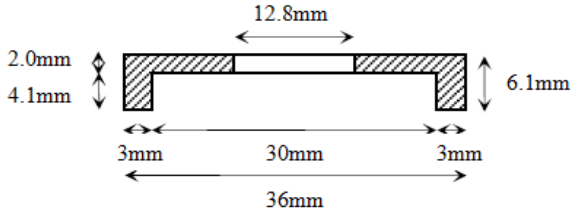

(c) Side View of Support Dimensions

Figure 3.10 Procedure used to control binder thickness

In order to evaluate the effect of anti-stripping additives on the bonding between binder and aggregate, treatments were applied to the aggregate substrate, which simulates asphalt mixtures treated with anti-stripping agents. This treatment was performed in such a way to approximate, as closely as possible, the amount of anti-stripping additive that was actually treated in the HMA mixture. For this process, total surface area of aggregates in the HMA mixture was first estimated based on the procedure described in Kandhal et al. (1998). The total surface area of a mixture can be calculated by using its gradation characteristic and surface area factors, which are multiplication factors of each sieve size. The result of total surface area is the sum of the surface area for each sieve size, which is in turn 4.13 m^2/kg. The total aggregate surface area can then be used to calculate the surface area per gram of each anti-stripping

additive, followed by a required mass of the anti-stripping additive to be treated on the aggregate substrate with the known surface area of the aggregate substrate. For a more uniform and an efficient treatment of the additive on the aggregate plate, a solution of 2 ml water and the required amount of additive was prepared and applied to the surface of the substrate. Remaining procedures for the sample fabrication are as follows:

- Apply the solution of water and additive to the surface of the aggregate plate for samples with treatment. This step is skipped for NF, the case without treatment;
- Heat the aggregate plate, the pull-stub, and binder at the mixing temperature;
- Using a clean silicone mold (fig. 3.11(a)), pour the binder in the mold (fig. 3.11(b) and fig. 3.11(c));
- Trim any extra binder using a spatula to obtain an identical binder volume for all cases (fig. 3.11(d));
- Place the silicone mold face down on top of preheated aggregate substrate (fig. 3.11(e));
- Wait until the sample is cooled down and remove the silicone mold;
- Place the metal supports around the binder (fig. 3.11(f));
- Place the preheated pull-stub gently on top of the binder, pressing against the supports to ensure the target film thickness (0.4 mm) (fig. 3.11(g));
- Let the sample cool to room temperature for at least 24 hours before the pull-off test for unconditioned samples (fig. 3.11(h)). For conditioned samples, wait at least 1 hour before the sample is subjected to water conditioning;
- After removing from the water bath, immediately test the sample.

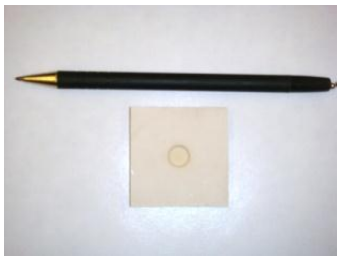

(a) Clean Silicone Mold

(b) Pouring the Binder in the Mold

(c) Binder in the Mold

(d) Trimming the Binder

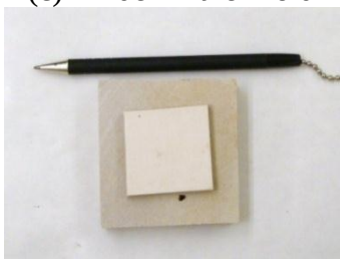

(e) Face-down Mold on Aggregate Plate

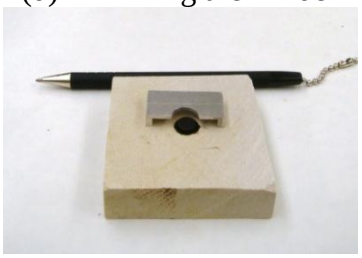

(f) Binder Sample with Support

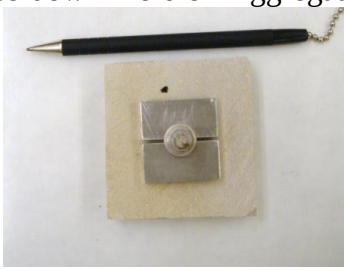

(g) Supports and Pull-Stub

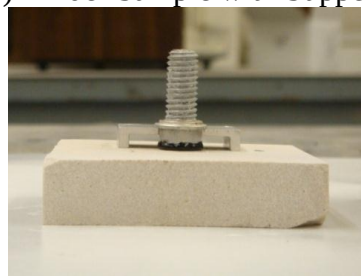

(h) Side View of a Prepared Sample

Figure 3.11 Sample preparation procedure

To perform the pull-off test using the PATTI, the piston is placed over the pull-stub and attached in the reaction plate by the threads of the pull-stub. Air pressure is transmitted to the piston through the pressure hose. A constant rate of pulling pressure, which is set in the PATTI pressure control panel, is applied to the sample, and test results in a form of tensile pressure vs.

testing time are recorded by a data acquisition system. A typical set of test results at different moisture conditioning levels is presented in figure 3.12.

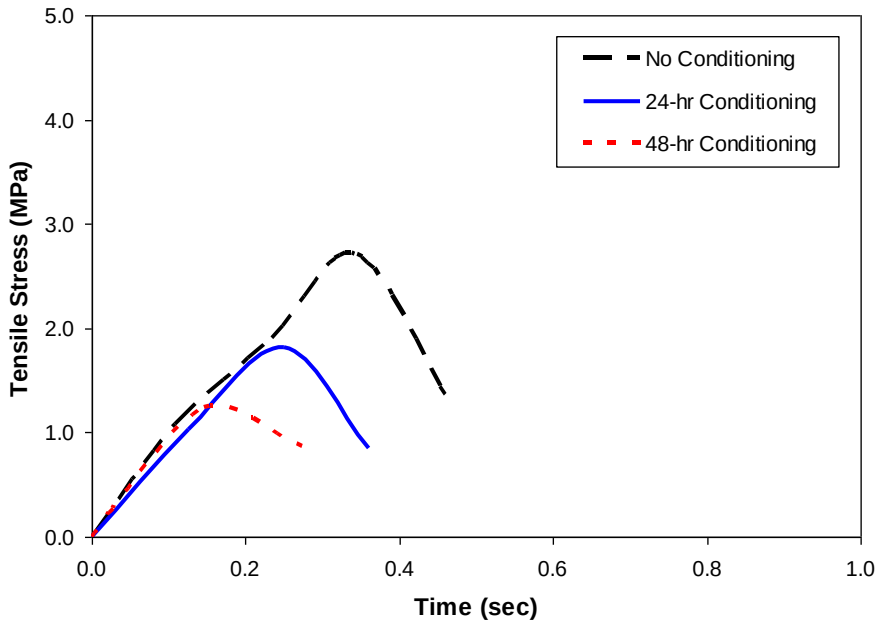

Figure 3.12 A typical set of test results from the pull-off PATTI test

If the tensile pressure exceeds the bond strength between the pull stub and a substrate, failure occurs in the sample. The pressure at failure (*BP*) is captured and transmitted to its pull-off tensile strength (*POTS*) by the following equation:

$$POTS = \frac{(BP * A_g) - C}{A_{ps}} \tag{3.2}$$

where: *POTS* = pull-off tensile strength (psi),

BP = burst pressure (psi),

A_g = contact area of gasket with relation plate (in^2),

C = piston constant (lb), and

A_{ps} = area of pull-stub (in^2).

Copeland (2007) utilized the PATTI to evaluate the bond strength between aggregate and asphalt binder using different modified binders. The asphalt binder was mixed to 200 μm glass beads in order to guarantee the film thickness. Then, the material was pressed between a glass substrate and a porous ceramic stub that allows water to migrate consistently through to the asphalt film. The pull-off tensile strength (*POTS*) was used as a measure of the adhesive characteristics of the asphalt binder. Moisture damage was induced by soaking in water, which appeared to be the most significant factor to the asphalt-aggregate bond strength. Test results were sensitive to binder modification.

Kanitpong and Bahia (2005) evaluated the adhesion and the cohesion failure of binders modified with anti-stripping agents and polymers to limestone and granite substrates using the PATTI. The samples were tested unconditioned and water-conditioned for 24 hours at 25°C. Test results demonstrated that binder characteristics and aggregate source are significant factors affecting moisture susceptibility. The authors concluded that adhesive properties improved when anti-stripping agents and polymers were added to the binder. The cohesive properties of binder did not change significantly with the addition of anti-stripping agents, while polymer-modified binders presented considerable changes in their cohesive properties.

It is noteworthy to mention that increasing numbers of researchers attempt to look for small-scale testing and analyses to better understand and predict the moisture susceptibility of asphalt materials. Test methods using compacted asphalt concrete samples are typically costly and time-consuming, and are limited in validating detailed moisture-damage mechanisms of HMA mixtures, because several mixture factors, such as mixture volumetric variables and aggregate geometric characteristics, are also involved. Therefore, recent studies have focused on local-scale (aggregate, binder, and their interface) analysis to investigate fundamental

characteristics of the binder-aggregate system (Kanitpong and Bahia 2005; Cho and Bahia 2007; Kim et al. 2008; Kringos and Scarpas 2008).

3.5 Numerical Modeling of Pull-off Testing

The objective of this effort is to further estimate the effectiveness of anti-stripping agents through a numerical modeling approach. Tensile stress-separation displacement data at the asphalt-aggregate interface resulting from the pull-off test were used to characterize the bonding-debonding potential of the interface to which different types of anti-stripping additives were applied. A sequentially coupled moisture diffusion–mechanical analysis was implemented into a commercial finite element software, ABAQUS, to predict the bond strength and progressive interfacial degradation due to the moisture diffusion followed by the application of mechanical pulling pressure. To model the adhesive fracture (i.e., debonding) at the binder-aggregate interface, the cohesive zone modeling (CZM) technique was incorporated into the model. This effort was expected to be suitable for evaluating moisture-damage mechanisms and effectiveness of anti-stripping additives in asphalt mixtures in a more scientific and fundamental manner.

3.5.1 Finite element mesh

Figure 3.13 shows a finite element mesh constructed to simulate the pull-off testing. The size of aggregate substrate is 25 mm long and 20 mm high, and the asphalt binder was placed on the aggregate plate, with a geometry of 15 mm long and 0.4 mm thick. Cohesive zone interface elements were inserted between binder and aggregate. Two-dimensional, four-node linear elements (DC2D4 in ABAQUS) were used for binder, aggregate, and interface elements to simulate the moisture diffusion process. For the mechanical loading and analysis, four-node plain strain elements (CPE4 in ABAQUS) were used for binder and aggregate. Zero-thickness cohesive zone elements (COH2D4 in ABAQUS) were employed to represent the interface

between the binder film and aggregate substrate. Aggregate was modeled as isotropic linear elastic material, and the asphalt binder was modeled as isotropic linear viscoelastic. The cohesive zone elements placed at the interface were modeled using the bilinear traction-separation relationship discussed in the next subsection.

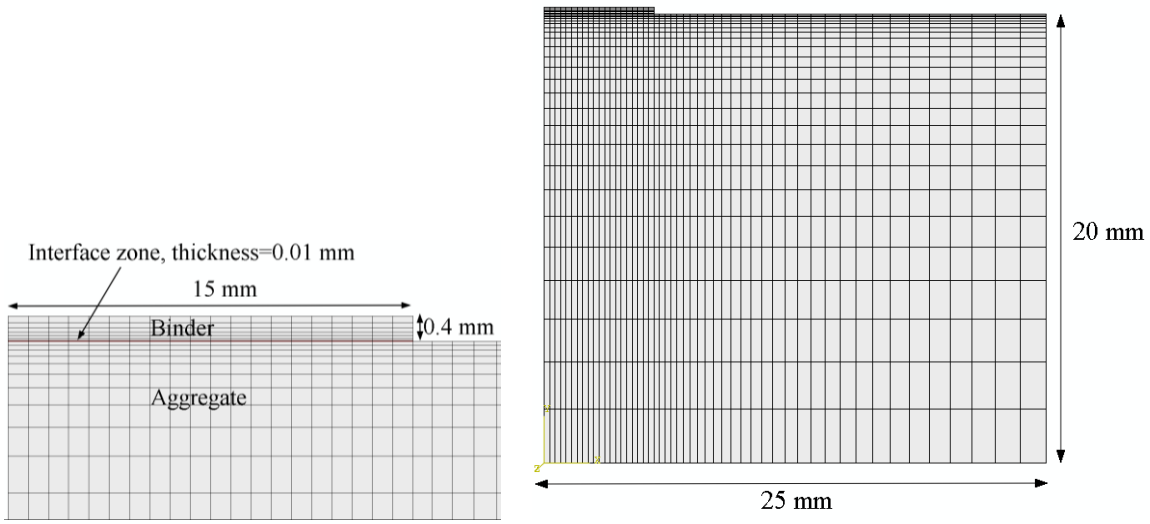

Figure 3.13 Finite Element Mesh

3.5.2 Modeling methodology: coupled moisture diffusion–mechanical loading

To conduct the sequentially coupled moisture diffusion–mechanical analysis scheme, the modeling consists of two processes. First, moisture diffusion is simulated, which results in moisture diffusion profiles of the sample. Second, the mechanical loading (pull-off pressure) to the sample is simulated before and during the moisture diffusion process. Therefore, the moisture diffusion profiles generated at the previous step are sometimes used as a prescribed condition of the mechanical loading simulation. It should be noted, that it was assumed for the modeling that the mechanical response of the system was dependent on the moisture diffusion processes

through the coupling of two analyses, but moisture diffusion was independent of the state of stresses within the system.

In order to characterize the moisture uptake and diffusion behavior, Fick's second law as expressed in equation 3.3 was used, since it has been widely used in modeling the diffusion in adhesively bonded structures (Hua et al. 2006).

$$\frac{\partial \phi}{\partial t} = D_d \frac{\partial^2 \phi}{\partial x^2} \tag{3.3}$$

where: ϕ = moisture concentration, and

D_d = moisture diffusion coefficient.

As expressed in the equation, moisture diffusion is governed only by the diffusivity coefficient with time, which infers that moisture absorption is not considered in the modeling. The moisture profile at each location within the sample is computed during the soaking time, as exemplified in figure 3.14. The figure presents the moisture profile of the binder-aggregate system after a 24-hour immersion in a water bath.

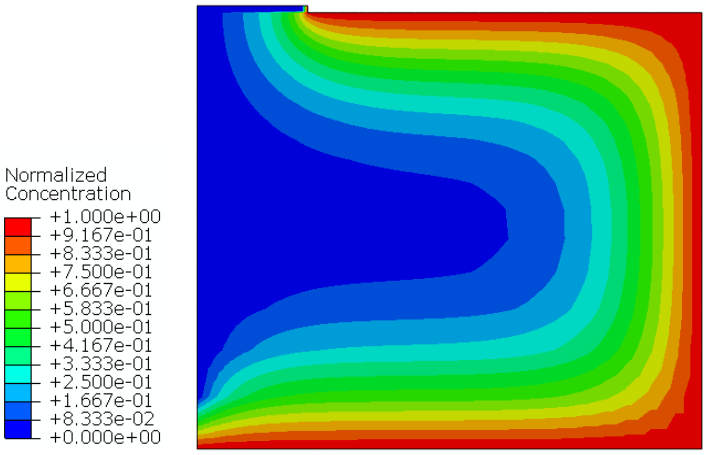

Figure 3.14 Moisture diffusion profiles after a 24-hr immersion

As mentioned earlier, the CZM was used to simulate the fracture process at the interface. This technique is an efficient approach to simulate crack initiation and propagation within a material or between two materials bonded together. Furthermore, CZM has also been successfully used to model the delamination of various composite materials under humid environments (Loh et al. 2003; Hua et al. 2006; Liljedahl et al. 2006).

Cohesive zone models regard fracture as a gradual phenomenon in which separation takes place across a cohesive zone (fracture process zone), and where fracture is resisted by cohesive tractions. Cohesive zone elements are placed between continuum elements to represent progressive separation of a material or between materials. The cohesive zone effectively describes the material resistance when material elements are being displaced.

CZM is typically expressed by a simple traction-separation relationship with several fracture parameters that represent the relationship between separation (δ) and traction (τ). The traction increases up to τ^o, denoted as cohesive strength at the beginning of separation, δ_o; then it decreases until it reaches a critical separation, δ_f and finally it becomes zero, as illustrated in figure 3.15. At this point, because the material is perfectly separated, no traction is transferred.

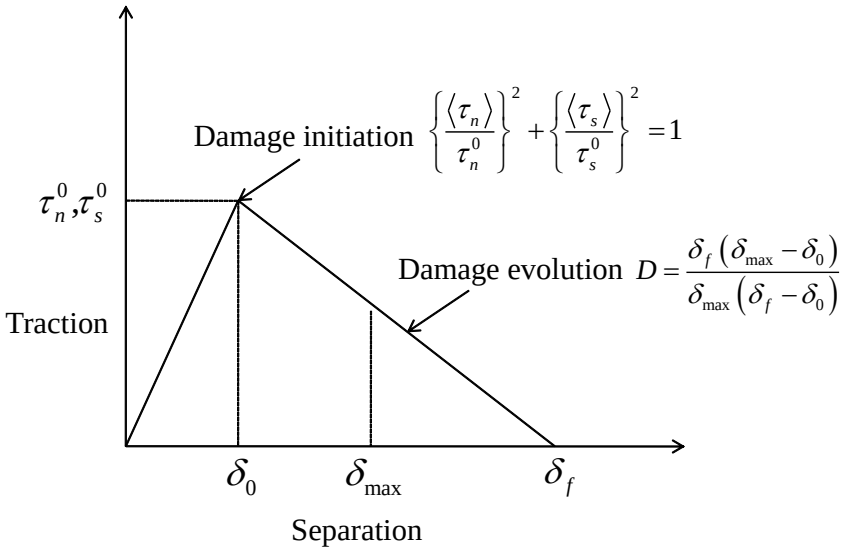

Figure 3.15 Bilinear cohesive zone model and its damage criterion

As presented in figure 3.15, damage initiates when a quadratic interaction function involving the nominal stress ratios reaches a value of unity. This criterion can be mathematically expressed as:

$$\left\{\frac{\langle\tau_n\rangle}{\tau_n^0}\right\}^2+\left\{\frac{\langle\tau_s\rangle}{\tau_s^0}\right\}^2=1 \tag{3.4}$$

where: τ_n and τ_s = normal and shear stresses in the cohesive zone element, and

τ_n^0 and τ_s^0 = peak values of the nominal stress and shear stress, respectively.

Progressive damage is a function of damage evolution parameter, *D*, which represents overall damage in the cohesive element. On the basis of an effective displacement, $(\delta_{\max}-\delta_0)$, which is the relative displacement when the traction is at its peak, the damage parameter can be defined as follows:

$$D = \frac{\delta_f \left(\delta_{\max} - \delta_0 \right)}{\delta_{\max} \left(\delta_f - \delta_0 \right)} \tag{3.5}$$

The cohesive zone traction is degraded from the original traction, as the damage parameter *D*, which is governed by the variation of separation displacement at the cohesive zone, increases. Therefore, the damage parameter value of unity implies that the corresponding cohesive element has completely failed. When compressive stress is applied, it is assumed that the cohesive zone is not subjected to damage. With that, cohesive zone stresses (normal and shear) with the damage parameter involved can be finally expressed as follows:

$$\begin{aligned} \tau_n &= \begin{cases} (1-D)\bar{\tau}_n & \bar{\tau}_n \geq 0 \\ \bar{\tau}_n, & \bar{\tau}_n < 0 \end{cases} \\ \tau_s &= (1-D)\bar{\tau}_s \end{aligned} \tag{3.6}$$

Figure 3.16 illustrates vertical stress contours of the binder-interface-aggregate system as the level of damage evolved during the pull-off loading process. Interfacial (adhesive) degradation followed by complete deboning can be successfully simulated by the use of cohesive zone elements.

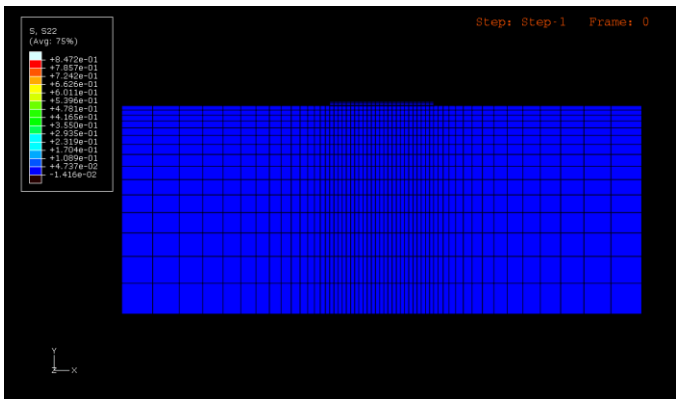

(a) Initial Stage

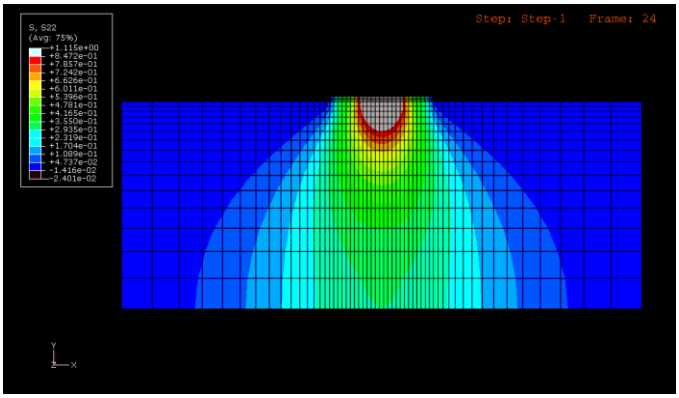

(b) Intermediate Stage

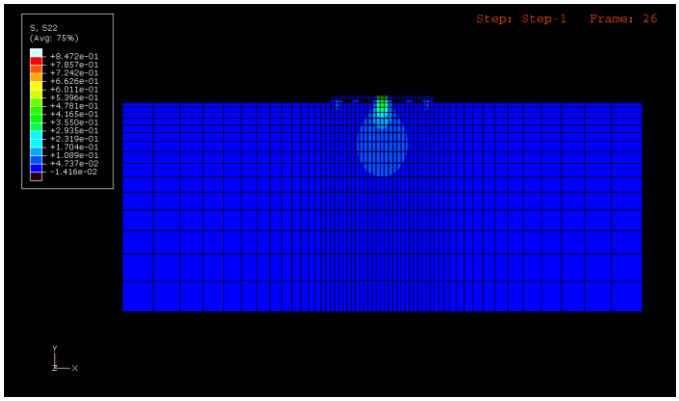

(c) Onset of Debonding

Figure 3.16 Vertical stress contour plots

Chapter 4 Results and Discussion

The Superpave mix designs of all six *SP5* mixes (NF, HL, FA, CM, HLB, and LS) were accomplished at UNL. Mix design results are presented in this chapter. Laboratory performance testing results from AASHTO T-283 and the APA under water are also presented and discussed in detail in this chapter. Results from two local-scale tests (the boiling water test and the pull-off test) to evaluate binder-aggregate bonding characteristics depending on the type of anti-stripping additives are also be presented and correlated with mixture performance test data. The finite element modeling of the pull-off testing was performed using ABAQUS, and simulation results are also presented and further discussed in this chapter.

4.1 Mix Design Results

Volumetric parameters and aggregate properties of each mix are shown in table 4.1. All *SP5* mixes were designed at UNL, and representative batches of each mix were sent to NDOR laboratories for validation. As can be seen in the table, mix volumetric properties and aggregate characteristics obtained from UNL laboratory satisfied NDOR *SP5* mix specifications.

Table 4.1 Volumetric mix properties and aggregate properties

Parameters	NDOR Specifications	Mixtures					
		NF	HL	FA	CM	HLB	LS
% V_a	4.0 ± 1.0	4.8	4.0	4.6	4.6	4.8	4.9
VMA	> 14	15.4	14.4	14.7	14.7	14.5	15.4
VFA	65-75	68.6	72.1	68.8	68.5	67.3	67.3
$\%P_b$	-	5.80	5.50	5.40	5.40	5.35	5.40
D/B	0.7 - 1.7	0.83	1.34	1.05	1.3	0.83	1.21
Gmm	-	2.427	2.430	2.440	2.444	2.443	2.433
G_{sb}	-	2.576	2.576	2.576	2.576	2.576	2.576
G_{mb}	-	2.343	2.363	2.360	2.358	2.357	2.341
CAA	> 95/90	96/96	96/96	96/96	96/96	96/96	96/96
FAA	> 45	45.2	45.2	45.2	45.2	45.2	45.2
SE	> 45	83	83	83	83	83	83
F&E	< 10	4	4	4	4	4	4

4.2 Performance Testing Resulting of Asphalt Concrete Mixes

4.2.1 AASHTO T-283 testing results

For each mix, three subsets (three specimens for each subset) compacted with 7.0% ± 0.5% air voids were tested. The first subset was tested in an unconditioned state, the second subset was subjected to partial vacuum saturation (degree of saturation of 70% to 80%) followed by one freeze-thaw (F-T) cycle, and the third subset was tested with the partial vacuum saturation and six F-T cycles. In the field, asphalt mixtures may experience many F-T cycles during their service life, which was simulated by introducing the multiple F-T cycling.

Figure 4.1 illustrates typical testing results that demonstrate testing repeatability. It also illustrates the fact that conditioned samples usually experience more moisture damage than unconditioned samples and, as expected, the multiple F-T cycling accelerates moisture damage. This acceleration results in substantial structural degradation of the HMA samples.

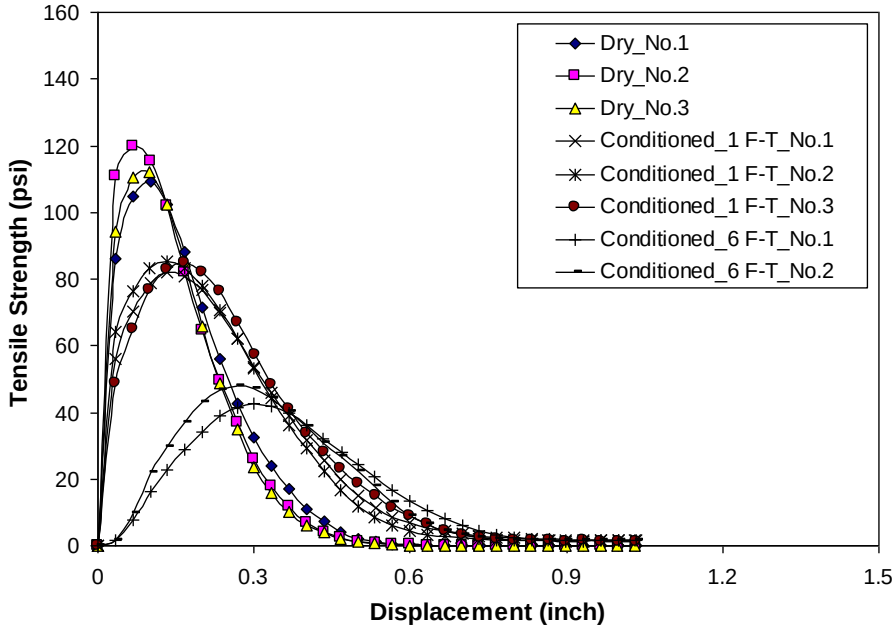

Figure 4.1 Typical AASHTO T-283 test results (Kim and Lutif 2006)

Figure 4.2 shows the average tensile strengths with the error bars of each mixture at three levels of conditioning: unconditioned, one F-T cycle, and six F-T cycles. Average tensile strength values of each mixture were then used to calculate tensile strength ratios (TSR) as follows:

$$TSR = \frac{TS_C}{TS_U} \qquad (4.1)$$

where: TS_C = average tensile strength of the conditioned subset, and

TS_U = average tensile strength of the unconditioned subset.

Averaged TSR values of each mix are plotted in figure 4.3. The TSR represents a reduction in the mixture integrity due to moisture damage. A minimum of 80% TSR has been typically used as a failure criterion.

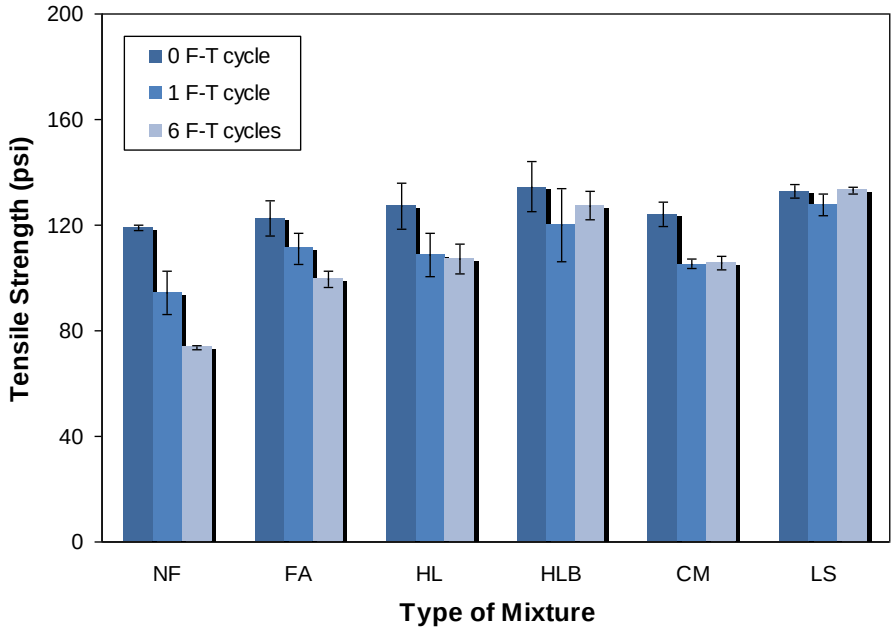

Figure 4.2 AASHTO T-283 test results

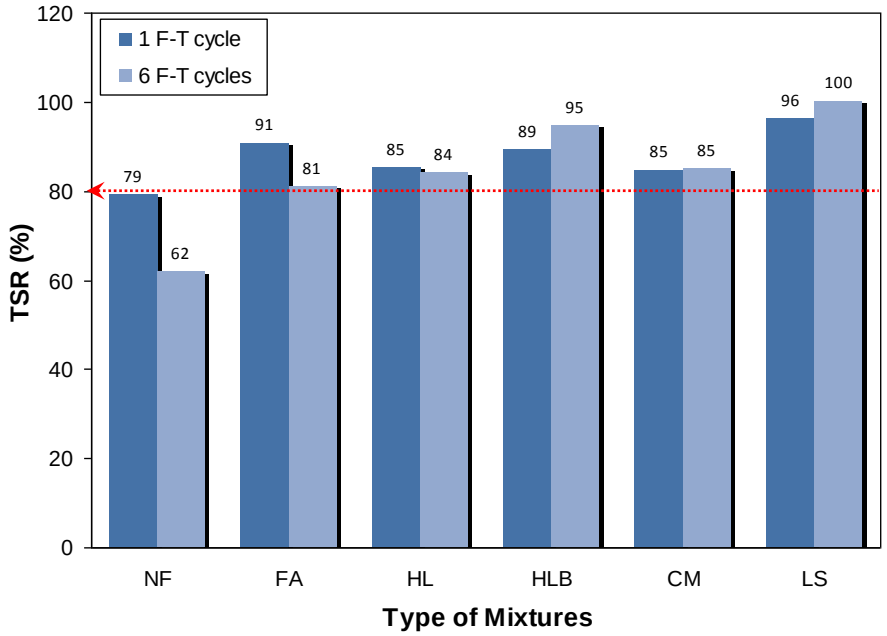

Figure 4.3 TSR results of each mixture

The addition of anti-stripping agents in the mixtures generally demonstrated positive effects with regard to moisture-damage resistance, particularly with six F-T cycles. The reference

(NF) mixture exhibited a TSR value close to the required limit when the mixture was subjected to only one F-T cycle; however, with six F-T cycles, the TSR value was close to 60%, representing failure by moisture damage. The TSR values from HL and CM were very similar for both conditioning levels. The FA mixture also performed similar to HL and CM mixes. Two other lime-associated mixtures (HLB and LS) seem to perform better than or at least similar to other treated mixtures. In summary, all treated mixtures passed the minimum required TSR value even after severe conditioning processes, and the untreated mixture performed fine with one F-T cycle. Test results imply that the *SP5* mixtures, where high-quality aggregates and polymer-modified binder are used, are fairly self-resistant to moisture damage without being treated with any anti-stripping additive. However, the use of anti-stripping additives in the mixture can still improve moisture-damage resistance, although any visible sensitivity among additives evaluated in this study has not been observed from the TSR estimation.

The synergistic effects of asphalt binder, aggregates, and additives on the moisture damage susceptibility can further be observed by the test results obtained from the previous NDOR research project (P564). In that study, a low-volume pavement mixture *SP2*, where low aggregate angularities and the unmodified asphalt binder PG 64-22 are necessary, was investigated for its moisture sensitivity by performing the AASHTO T-283 test. The APA test under water for various mixtures with different anti-stripping additives (hydrated lime for the AASHTO T-283 test, and hydrated lime and fly ash for the APA test) was also performed. For consistency with this project, the same sources of aggregates blended with an identical gradation were used, and 1% of additive by total weight of aggregates was added to the mixture. The values of TSR from the *SP2* mixes were 69% and 77% after one F-T cycle, and 11% and 49% after six F-T cycles, for the untreated (control) mix and hydrated lime–treated mix, respectively.

The effect of hydrated lime was significant and even more impressive when the mixes were subjected to multiple F-T cycling. The mixes without lime treatment experienced severe damage with multiple F-T cycles, which is not true of the *SP5* mixtures, as shown in figure 4.3. For a clearer comparison between *SP2* and *SP5* test results, figure 4.4 is introduced. Clearly, the effects of binder and aggregate quality on the overall mixtures' resistance to moisture damage can be captured from the figure.

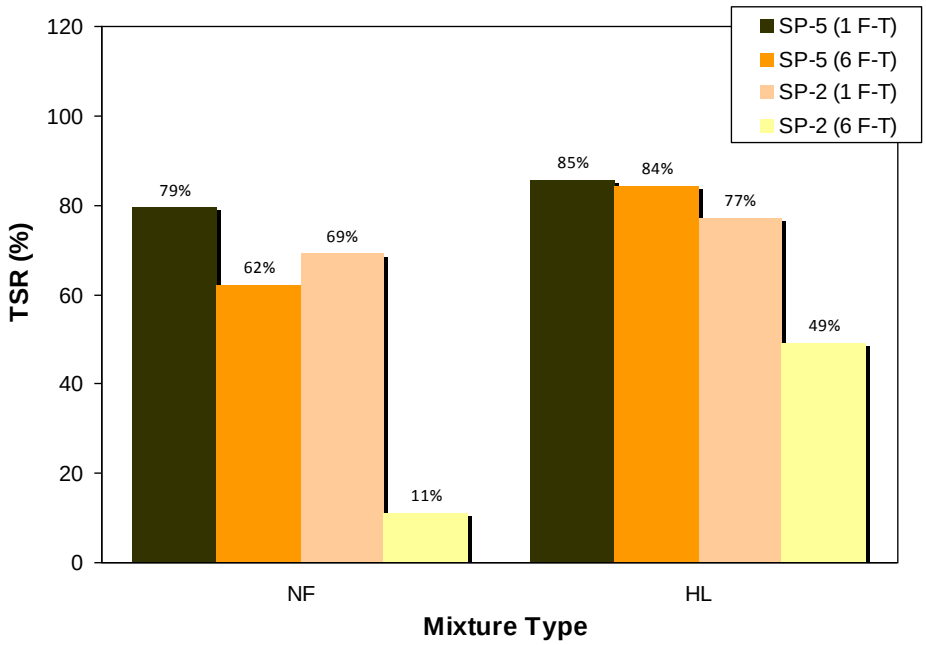

Figure 4.4 Combined AASHTO T-283 results from *SP2* and *SP5* mixtures

4.2.2 APA testing results

The APA testing was conducted on pairs (up to three) at a time using gyratory-compacted asphalt concrete specimens of 75 mm high with 4.0 ± 0.5% air voids. In the case that an APA specimen demonstrates deeper than 12 mm rut depth before the completion of the 8,000 cycles, the testing was manually stopped to protect APA testing molds and the corresponding number of

strokes at the 12 mm rut depth was recorded. Testing was conducted at 64ºC. In order to evaluate moisture susceptibility, the test was conducted under water. The water temperature was also set at 64ºC. The APA specimens were preheated in the APA chamber for 16 hours before testing. The hose pressure and wheel load were 690 kPa and 445 N (100 psi and 100 lb), respectively.

Figure 4.5 presents the APA performance-testing results of all six *SP5* mixes. As shown, the rut depth values after 8,000 cycles did not differ from mixture to mixture. All mixes presented a satisfactory performance according to the typical 12 mm failure criterion. High-quality mixture constituents (angular aggregates and polymer-modified binder) in the *SP5* mixtures resulted in good rutting performance with no significant sensitivity among mixtures, which was also observed from AASHTO T-283. APA testing could not capture the effect of the anti-stripping agent in the mixtures.

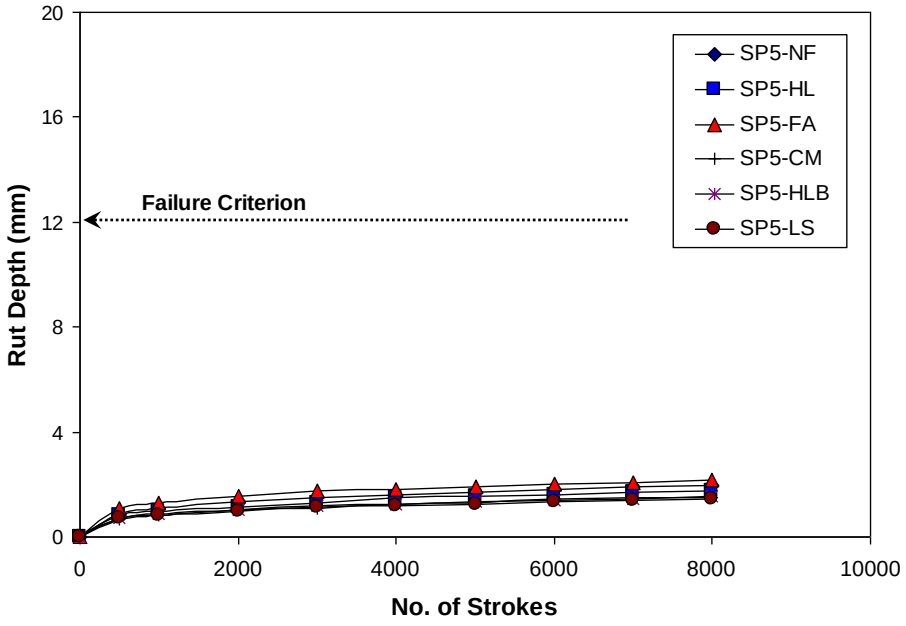

Figure 4.5 APA test results (*SP5* mixtures)

As mentioned earlier, the previous study also performed the APA test for *SP2* mixes treated with different additives: dry hydrated lime, lime slurry, and fly ash. The untreated control mix reached a 12 mm rut depth after 3,500 strokes, indicating premature failure of the mix. Mixtures treated with hydrated lime passed the failure criterion with a rut depth of approximately 5 mm and 6 mm after 8,000 strokes for dry lime and lime slurry, respectively, implying that the addition of hydrated lime improved the resistance of mixtures to the moisture damage. Mixtures treated with fly ash also performed very well.

Similar to figure 4.4, APA test results of *SP2* mixes from the previous research project and the *SP5* mixture results from this study are all combined and presented in figure 4.6. Several important observations can be extracted from the figure. By comparing the APA performance from the untreated *SP2* mixtures to the untreated *SP5* mixtures, the mechanical contribution of the polymer-modified binder and higher-angularity aggregates to the rutting-related moisture-damage resistance could again be verified. Anti-stripping effects of all three additives (hydrated lime, lime slurry, and fly ash) were positive and similar, while no dramatic impact was presented when they were added in the high-quality HMA mixtures.

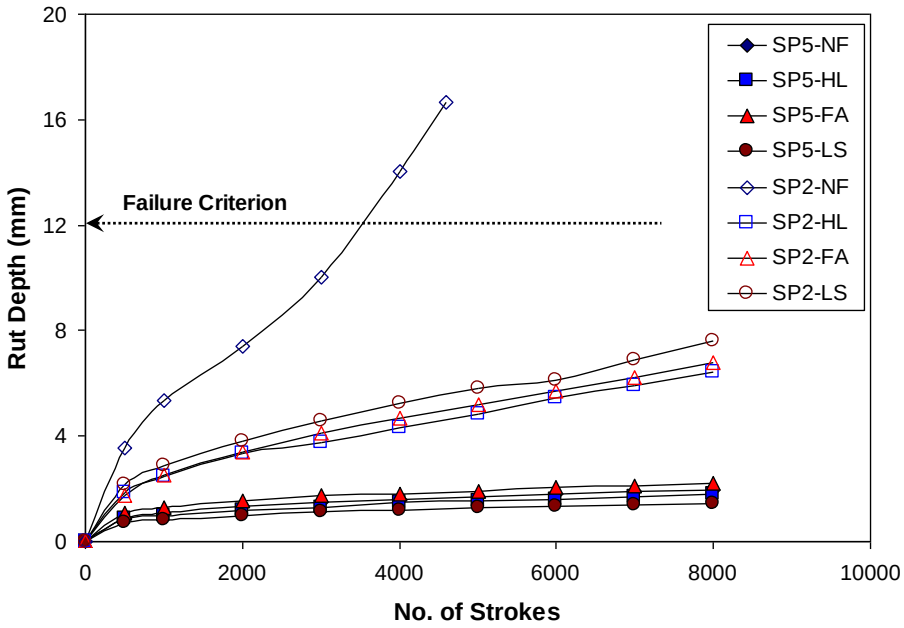

Figure 4.6 Combined APA test results from *SP2* and *SP5* mixtures

4.3 Local-scale Test Results

Test results from the two types of asphalt concrete mixtures (*SP2* and *SP5*) demonstrated the significant role of asphalt binder to the moisture-damage resistance as anti-stripping additives contribute to the adhesion between binder and aggregate. In fact, the effect of anti-stripping additives was not clearly seen from the mixtures with polymer-modified binder. To better understand the material-specific (i.e., binder-dependent and additive-dependent) moisture-damage characteristics particularly related to the adhesive bonding potential within the binder-aggregate system, two local-scale tests (the boiling water test and the pull-off test using a PATTI device) were performed and test results are presented here. Local-scale tests are believed to provide a better and more detailed insight into the adhesive fracture behavior due to moisture attack. Furthermore, results from the local-scale tests can be correlated to the performance results from the asphalt concrete mixture level.

4.3.1 Boiling water test results

In order to capture the effect of anti-stripping agents and binders, two binders (PG 64-22 and PG 70-28) and three additives (HL, FA, and CM) were considered. A reference case without any treatment of the additive was also tested to be compared with cases that are treated with one of the anti-stripping additives.

Each loose HMA mixture was subjected to boiling water for 10 minutes, and the percentage of asphalt coating remaining from the initial reference condition (before testing) was visually estimated by investigators to quantify the level of degradation due to moisture damage. As an example, figure 4.7 presents pictures taken from control cases (NF) mixed with binders PG 70-28 and PG 64-22, respectively, after the testing, and table 4.2 summarizes the average values (in percentage) given by three investigators.

(a) PG 70-28 (b) PG 64-22

Figure 4.7 Pictures taken from reference cases (NF)

Table 4.2 Boiling water test results (visual analysis)

Mixture	Visual Analysis (%)	
	PG 64-22	PG 70-28
NF	60	95
HL	75	95
FA	75	95
CM	70	95

In an attempt to estimate the test in a more objective manner than the subjective visual rating by the investigators, a digital image analysis of photographs taken for each mixture using a digital camera was conducted. Each picture was cropped to a consistent size and then transformed to a black-and-white image by applying the same level of threshold. The black area represents the aggregates covered with asphalt binder, while the white portion represents aggregates or spots in the aggregates with stripping. In order to calculate the area of each portion, the image analysis software, ImageTool was used. ImageTool quantifies each portion by counting the number of pixels corresponding to each color and provides the percentage of black and white pixels. Figure 4.8 shows the cropped original images and their transformed images in black and white for the reference (NF) mixtures with two different binders: PG 64-22 and PG 70-28.

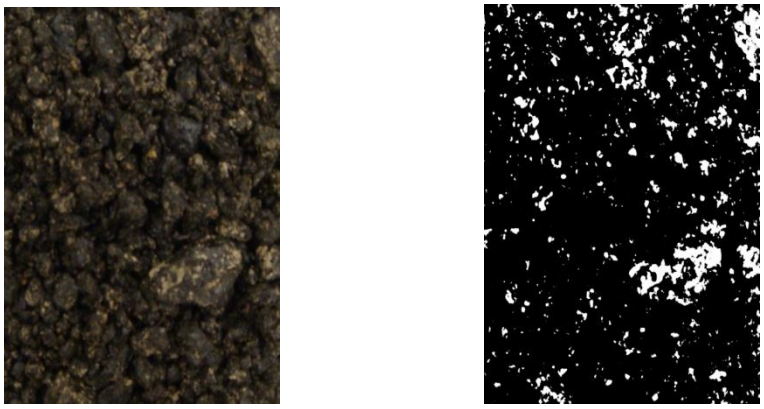

(a) PG 64-22 before Treatment (b) PG 64-22 after Treatment

(c) PG 70-28 before Treatment (d) PG 70-28 after Treatment

Figure 4.8 Digital image analysis with reference mixture (NF)

Analysis results are plotted in figure 4.9. Before making any conclusions from the figure, it should be noted that the values presented in the figure are influenced by several factors related to image processing, such as the level of threshold applied. In other words, one cannot affirm that the percentage of white portion is a real value of stripping. Factors can change the results of image analysis; however, a relative ranking among mixtures can still be made in an objective manner, because the identical factors are applied to all mixtures compared.

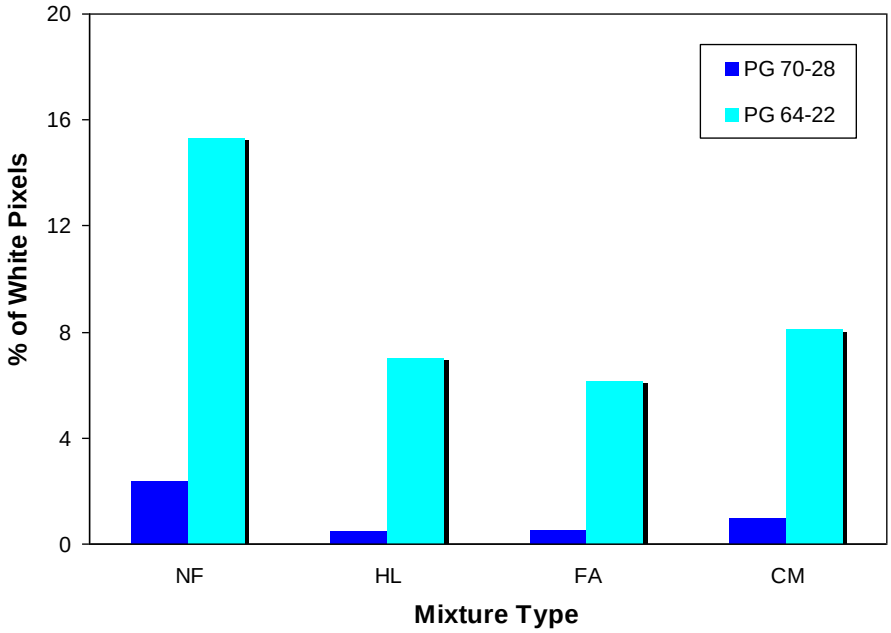

Figure 4.9 Digital image analysis results from the boiling water test

Results from the digital image analysis are in good agreement with the results from the visual analysis in that asphalt binder PG 64-22 was much less resistant to moisture damage than binder PG 70-28, and the effect of additives was more visible from the mixtures with binder PG 64-22 than the mixtures with PG 70-28. The CM mixture showed slightly more stripping potential than the HL and FA mixtures. Boiling water test results are quite consistent with observations from the two mixture-level performance tests.

4.3.2 Pull-off test results

The PATTI allows the sample to be conditioned in water. Therefore, moisture damage to the materials and their interface can be investigated and compared using different substrates, binders, and additives. For the pull-off testing, two binders (PG 64-22 and 70-28) were glued to a sandstone substrate with a total of four interface treatment strategies: treatment with hydrated lime, fly ash, and cement, and without treatment. Each case was tested at three moisture-

conditioning steps: 0-hour, 24-hour, and 48-hour conditioning in a water bath at 25°C (77°F). Unconditioned samples (i.e., 0-hour conditioning) were kept inside a dry chamber at the same temperature, 25°C (77°C), applied to the conditioned cases, to maintain equal testing conditions. For each case, at least three samples were tested at a constant pressure rate. Figures 4.10 and 4.11 present the average pull-off tensile strength and its variation marked by error bars.

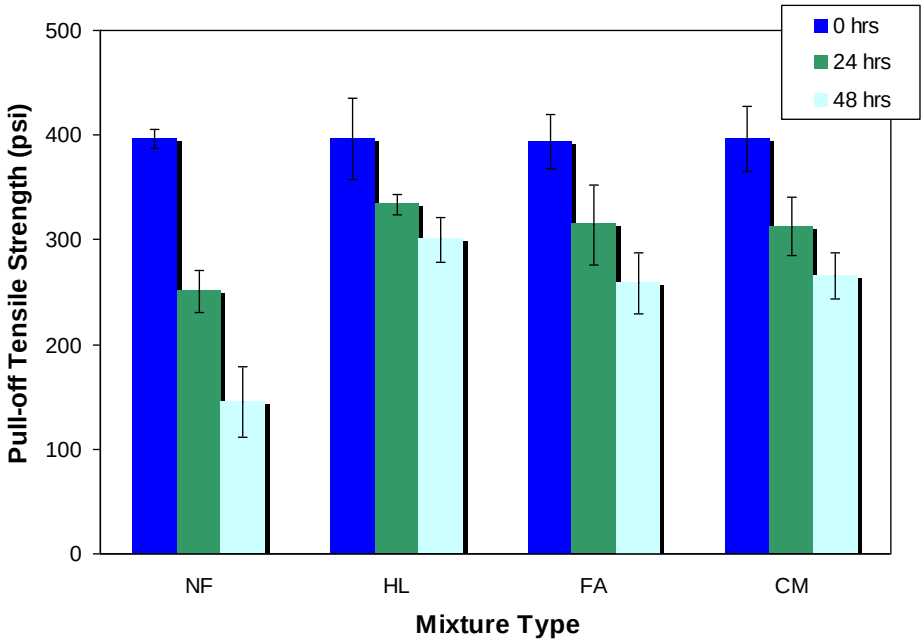

Figure 4.10 Pull-off test results from mixtures with binder PG 64-22

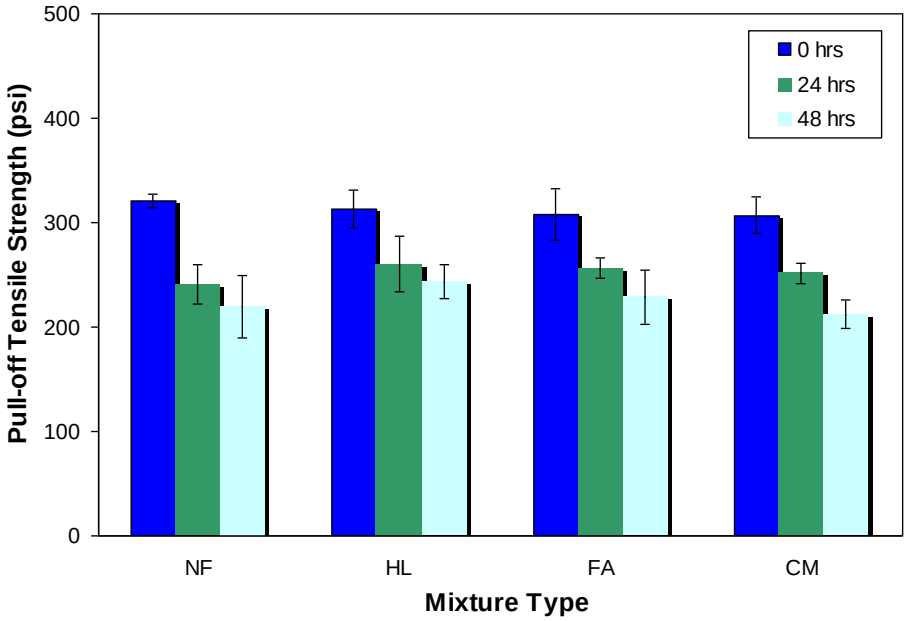

Figure 4.11 Pull-off test results from mixtures with binder PG 70-28

Tensile strength data shown in figures 4.10 and 4.11 can be used to calculate the tensile strength ratios (hereafter it is called PO-TSR: pull-off tensile strength ratio, to be distinguished from the TSR value of AASHTO T-283 testing) at the two different levels of moisture conditioning (24-hour and 48-hour). Table 4.3 summarizes the ratios.

Table 4.3 PO-TSR values

Binder	Conditioning Time (hours)	PO-TSR (%)			
		NF	HL	FA	CM
PG 70-28	24	75	83	83	82
	48	68	78	74	69
PG 64-22	24	63	84	80	79
	48	37	76	65	67

As expected, all cases suffered from damage due to the moisture conditioning, and the level of damage increased as the conditioning time increased. The table clearly demonstrates that the polymer-modified binder contributed to an increase in moisture-damage resistance, which has been identically observed in other tests. The effect of binders was even more impressive when the samples were subjected to longer moisture conditioning. The PO-TSR values from the reference mixture (NF) after a 48-hour conditioning were 68% from the sample with the PG 70-28 binder, but reduced to 37% when the unmodified binder was used. One more interesting thing that can be seen from the table is that additives in the mixtures play an important role in reducing stripping potential, which can be captured from the fact that PO-TSR values were not quite dependent on the type of binder when the samples were treated with additives. Even if it may not be conclusive, comparing only cases with treatment, hydrated lime seems to perform slightly better than other additives, particularly with longer conditioning time. There was no remarkable difference between two additives (fly ash and cement).

The pull-off test can also identify the type of failure, either adhesive or cohesive. According to a study by Kanitpong and Bahia (2005), when more than 50% of the aggregate is exposed from the debonding process between aggregate plate and binder film, the failure can be categorized as adhesive failure; otherwise, it is considered cohesive failure. As exemplified in figure 4.12, unconditioned samples typically presented cohesive failure in most cases, while adhesive fracture (fig. 4.12(b)) was more frequent from samples with 48-hour conditioning, which clearly implies that the presence of water caused a reduction in the bond strength between aggregate and binder.

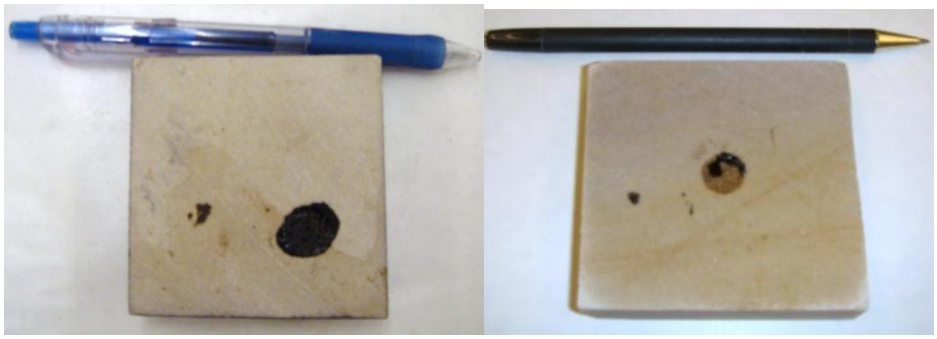

(a) Cohesive Failure (b) Adhesive Failure

Figure 4.12 Type of failure

The local-scale pull-off test results and global-scale (asphalt concrete mixture scale) test results from the AASHTO T-283 exhibited a close correlation on the tensile strength values among mixtures, as figure 4.13 presents a good linear relationship between two data sets with a R^2-value of 0.75. Only test data from unconditioned samples were included in the figure at this point, since the moisture-conditioning method for the AASHTO T-283 was not identical to the conditioning used for the pull-off testing.

Overall, performance test results of asphalt concrete samples appear to be strongly linked to small-scale mixture component characteristics. Evaluation of component characteristics, such as the adhesive fracture potential between binder and aggregate, aided to identify moisture-damage mechanisms and their impacts on pavement performance in a more fundamental manner. Use of component properties and characteristics will be significantly beneficial, since testing of mix components is much more economical and efficient than the testing of asphalt concrete samples. Additionally, component information can also be simply used to judge (or potentially predict) HMA performance based on the strong relationships between component characteristics and mixture performance.

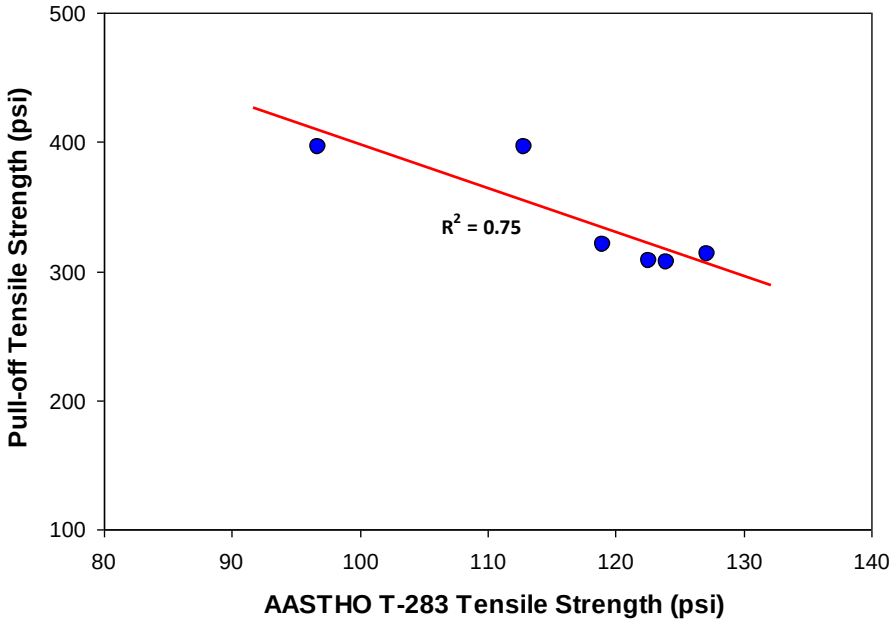

Figure 4.13 Relationship between two scale test results

4.4 Numerical Model Simulation Results

As introduced earlier, the effectiveness of anti-stripping additives on moisture damage was further characterized through the numerical simulation of the pull-off testing. The pull-off test provided the tensile stress vs. loading time (or corresponding displacement) spectrum and its peak value (pull-off tensile strength) at the binder-aggregate interface to which different anti-stripping additives were applied. The sequentially coupled moisture diffusion–mechanical analysis facilitated the progressive degradation of binder stiffness through the moisture diffusion, as well as the adhesive deterioration with fracture of binder-aggregate interface using a cohesive zone model. This section presents model simulation results and further related discussion.

4.4.1 Materials and their properties (model inputs)

To better characterize the effectiveness of anti-stripping additives from the pull-off tests, test results of samples with only the unmodified binder PG 64-22 and two additives (hydrated

lime and fly ash) were selected for the modeling, since they exhibited sensitive behavior to the level of moisture conditioning. Test results obtained from the samples fabricated with binder PG 70-28 were not considered here, because the effect of additives was not clear. For the aggregate substrate, sandstone was selected.

To conduct the moisture diffusion simulation, diffusion coefficients of each material (i.e., sandstone substrate, asphalt binder, and interface) are necessary as model inputs. Table 4.4 lists moisture diffusion coefficients, which were chosen from open literature (Kringos et al. 2007).

Table 4.4 Moisture diffusion coefficients employed for the modeling

Materials	Diffusivity Coefficient (mm^2/sec)
Aggregate (sandstone)	$1.6x10^{-4}$
Binder (PG 64-22)	$2.5x10^{-8}$
Interface	$2.5x10^{-8}$

In the mechanical analysis for the simulation of pull-off loading, a linear viscoelastic response was considered to describe the behavior of binder film, and linear elastic response was assumed to model the behavior of aggregate substrate. Table 4.5 shows the mechanical material properties of aggregate and binder. The viscoelastic properties of the binder shown in the table were obtained from the relaxation tests using a DSR at 25^oC reference temperature, while elastic properties of aggregate (E and ν) were reasonably assumed.

Table 4.5 Mechanical material properties of aggregate and binder

Elastic Material Properties		
Aggregate	E (MPa)	υ
	50,000	0.35
Linear Viscoelastic Material Properties		
Prony series parameters for binder (PG 64-22)	Shear modulus, G_i (kPa)	Relaxation time, ρ_i (sec)
	20,020.96	0.0014
	4,129.56	0.014
	826.70	0.14
	96.37	1.4
	12.12	14
	0.5	∞

The model simulates moisture damage in two ways: (1) degradation of binder stiffness due to moisture diffusion over time, and (2) deterioration and failure of binder-aggregate interface subjected to the moisture saturation followed by pullout loading. These two processes are typically represented as cohesive and adhesive damage, respectively. The first type of damage (cohesive damage) was simulated by decaying the linear viscoelastic properties of the binder as a function of the level of moisture saturation. To that end, a series of simulations and its sensitivity analysis was performed using several potential decaying functions (linear, exponential, etc.). Simulations demonstrated no significant difference on the overall damage characteristics among decaying functions tested. Therefore, a simple linear degradation was chosen in this study.

More attention was given to the second type of damage (adhesive fracture at the interface) in this study, since the characterization of the effects of additives is directly related to the interfacial adhesive fracture behavior. As mentioned earlier, the CZM, which is presented in equations 3.4 to 3.6 and is graphically illustrated in figure 3.15, was used to represent initiation

and evolution of adhesive failure at the interface between the aggregate substrate and asphalt binder.

The interfacial CZ properties (τ^o, δ_o, and δ_f) of each sample (NF, HL, and FA) were first obtained by a matching process between the experimental results at dry condition (before soaking) and their numerical model simulations. Table 4.6 presents the CZ properties of each sample before moisture damage was initiated. The dry-condition CZ properties were then degraded as the moisture conditioning continued because of moisture saturation.

Table 4.6 CZ properties of each sample at dry condition

Sample	τ^o (MPa)	δ_o (mm)	δ_f (mm)
NF	2.65	0.14	0.40
HL	2.77	0.17	0.43
FA	2.67	0.15	0.35

The reduction of CZ tensile strength due to moisture saturation can then be formulated by equation 4.2. The equation represents how the interfacial property (τ^o in this case) degrades as the level of moisture conditioning evolves by simply relating the normalized interface (CZ) strength to the normalized value of moisture saturation through the exponential relationship.

$$\frac{\tau_{wet}^0}{\tau_{dry}^0} = \exp\left[-k\left(\frac{\phi}{\phi_{sat}}\right)^n\right] \tag{4.2}$$

where: τ_{dry}^0 = CZ tensile strength at unconditioned (dry) stage;

τ_{wet}^0 = CZ tensile strength at certain level of moisture conditioning (wet);

ϕ = degree of saturation at certain level of moisture conditioning;

ϕ_{sat} = degree of saturation at the fully saturated level; and

k and *n* = model parameters.

The model parameter *k*-value in the equation determines the bond strength remaining at complete moisture saturation. As illustrated in figure 4.14, when the k-value is 1.0, approximately 37% of dry-condition bond strength remains, even if the sample is fully saturated. When the k-value increases (such as from 1.0 to 5.0 as shown in the figure), the remaining bond strength significantly decreases and approaches zero as the level of saturation becomes greater.

Another model parameter, the exponent *n*-value, determines the shape of degrading trend, as presented in figure 4.14 with three different *n*-values (0.5, 1.0, and 5.0). As the *n*-value decreases, samples lose interfacial strength at an early stage in a more sensitive manner than the case with a higher *n*-value. Thus, the *n*-value can be used as an indicator to quantitatively assess the effectiveness of anti-stripping additives treated at the binder-aggregate interface.

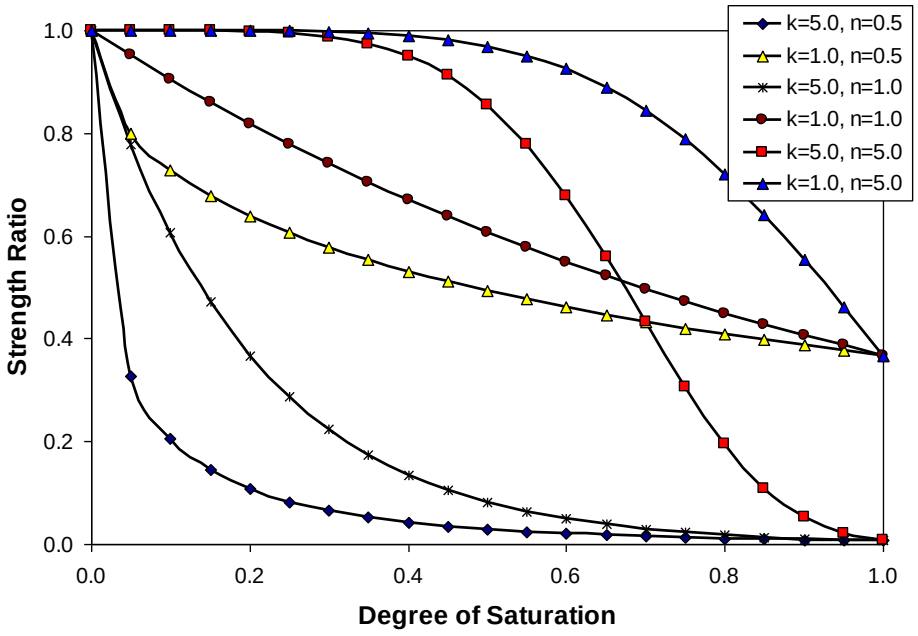

Figure 4.14 Strength ratio vs. degree of saturation

4.4.2 Model simulation and results

The moisture profile in the sample was generated by allowing moisture to diffuse into the binder-interface-aggregate system for 24 hours and 48 hours, as presented in figure 4.15. As would be expected, moisture diffuses more into the media with an increase in soaking time. As moisture diffuses more into the sample, it is expected that the binder will becomes more compliant based on the linear stiffness degradation scheme, and the interface is subjected to greater damage potential due to its higher percentage of moisture saturation, which will lead to poorer performance under the mechanical pull-off loading.

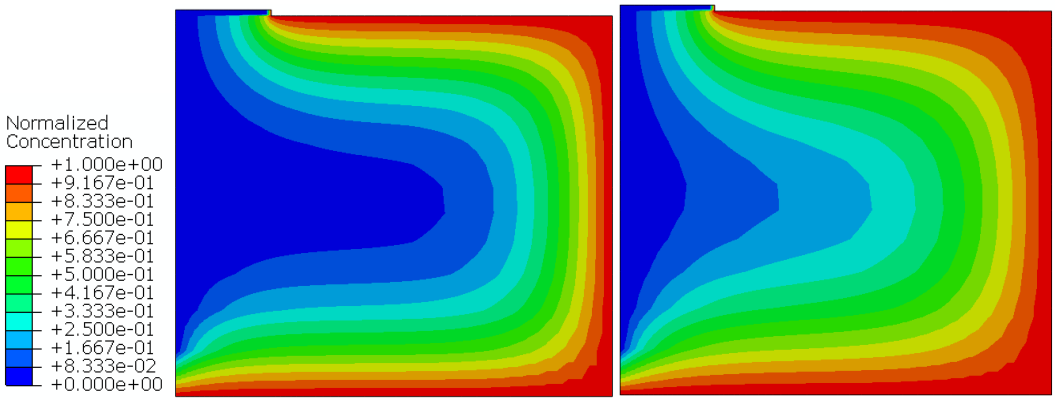

(a) 24-hours (b) 48-hours

Figure 4.15 Moisture diffusion profiles at the soaking time

Along with the moisture diffusion simulation, mechanical loading of the pull-off test was modeled by using the same finite element mesh. However, the diffusion-based elements (i.e., DC2D4 in ABAQUS) were replaced with mechanical-based elements (CPE4 solid elements for binder and aggregate substrate, and COH2D4 elements for the interfacial cohesive zone). During this coupling process, the mechanical properties, such as the viscoelastic properties of binder and fracture properties of cohesive zone, are degraded corresponding to the prescribed profile of

moisture saturation (as shown in fig. 4.15). In other words, a linear degradation of relaxation modulus to the level of moisture saturation was applied to the viscoelastic binder properties, and equation 4.2 was implemented in the model to represent damage evolution at the interface due to the progressive moisture saturation. A series of model simulations for each sample (NF, HL, and FA) at three different moisture-conditioning levels (dry, 24-hr soaking, and 48-hr soaking) were repeated by varying two model parameters (*k*- and *n*-value) until model simulations presented a good agreement with pull-off test results. Model parameters found can then be used to assess the effectiveness of additives and their contribution to the anti-stripping potential.

Figure 4.16 illustrates a comparison between model simulations and test results typically observed from all three cases (NF, HL, and FA). As shown, model simulations could successfully predict the progressive sample degradation with increasing moisture conditioning, and generally match well with the experimental data over the whole process of damage initiation to complete fracture.

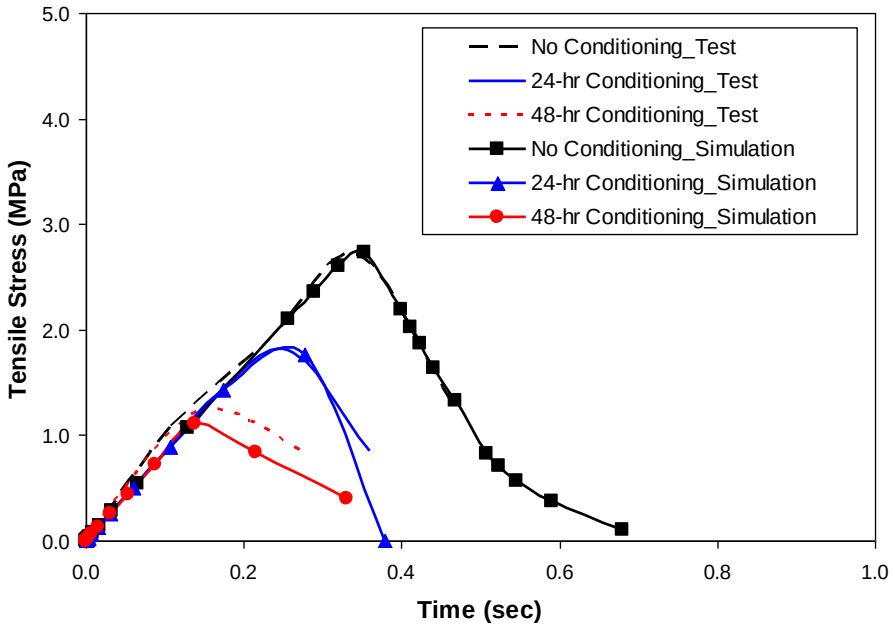

Figure 4.16 Model simulations vs. test results (NF Samples)

The predicting power of the model is further demonstrated in figure 4.17. It compares the maximum bond strength values directly monitored from the testing to the simulated values. Finite element predictions generally matched very well with experimental results, which implies that the model parameters (original CZ properties and their degradation characteristics by two parameters: *k*- and *n*-value) were defined properly. It can also be observed from the figure that the bond strength of each sample was initially very similar, but degraded in a very different way because of the additives. Anti-stripping additives clearly contributed to the higher resistance to moisture damage, and hydrated lime–treated samples presented the best performance.

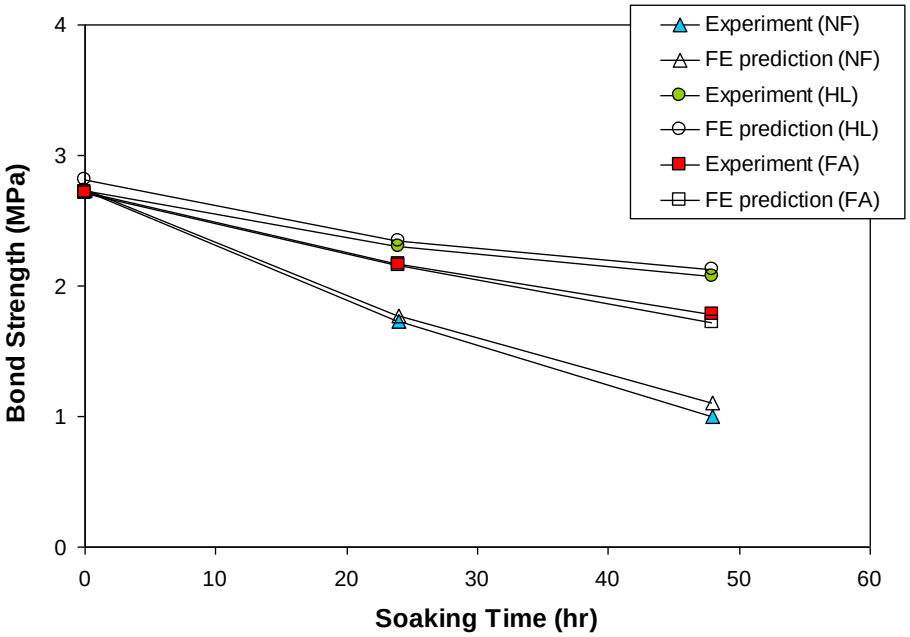

Figure 4.17 Comparison of bond strengths

Finally, figure 4.18 presents the degradation curves generated by equation 4.2 and its model parameters found from the matching process aforementioned. A constant *k*-value of 4.6, which implies that 99% of interfacial bond strength is diminished at the fully saturated condition,

was applied to all cases for this study, because the remaining bond strength at 100% moisture saturation could not be obtained using current data. With the constant *k*-value, corresponding *n*-values that provide a good agreement with test results was determined.

The *n*-value physically implies the rate of degradation. As the *n*-value decreases, the system is potentially more sensitive to moisture damage. Each degradation curve basically characterizes how each interface system between binder and aggregate responds to moisture. Ranking of interface systems to the moisture-damage resistance can be made simply by comparing the *n*-values. Once again, the positive effect of anti-stripping additives, HL and FA, appeared in the figure.

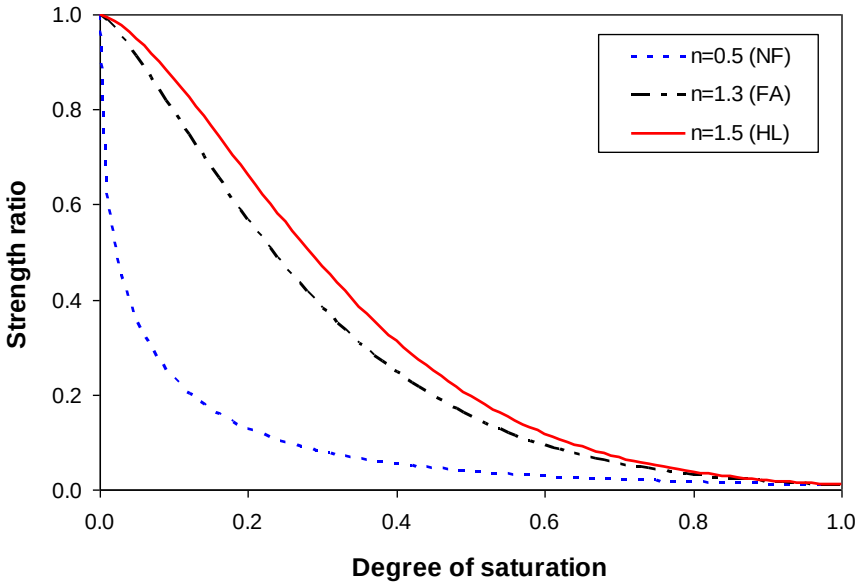

Figure 4.18 Comparison of degradation characteristic curves

Chapter 5 Summary and Conclusions

Performance changes and fundamental material characteristics associated with moisture damage due to various anti-stripping additives in HMA mixtures were studied through various experimental approaches and a numerical simulation. Three additives (i.e., one reference additive, hydrated lime, and two alternative additives: fly ash and cement) were investigated by adding them into two types of mixes (*SP2* for low-traffic-volume roadways and *SP5* for high-traffic-volume roadways) where two different asphalt binders (i.e., PG 64-22 for the *SP2* mix and polymer-modified binder PG 70-28 for the *SP5*) were used. Two asphalt concrete mixture scale performance tests, the AASHTO T-283 and the APA under water, and two local-scale mixture constituent tests, the boiling water test (ASTM D 3625) and the PATTI pull-off test, were conducted to characterize the effects of binder-specific anti-stripping additives on the binder-aggregate bonding potential in mixtures. The pull-off tensile strength tests were then numerically modeled through the finite element technique incorporated with the cohesive zone modeling approach to seek more fundamental scientific insights into the effect of each anti-stripping additive on the overall moisture-damage resistance. Outcomes from this research project were then incorporated with research findings from the previous NDOR research project (P564) on moisture damage in asphalt mixtures/pavements to draw more comprehensive and general conclusions. The following conclusions and suggested follow-up studies can be drawn:

5.1 Conclusions

- The AASHTO T-283 test results presented that all treated mixtures performed well even after severe moisture-conditioning process, while the untreated mixture did not pass the requirement with six F-T cycles. Test results, however, imply that the *SP5* mixtures, where high-quality aggregates and polymer-modified binder are used, are fairly self-resistant to

moisture damage without being treated with any anti-stripping additive, and did not show any visible sensitivity among additives, whereas the effects of additives and their sensitivity were significant in the *SP2* mixes that use the unmodified binder PG 64-22 and low-quality aggregates.

- Results from the APA test under water were consistent with results from the AASHTO T-283, in that the rut depth values of *SP5* mixes did not present any dramatic impact from additives and their sensitivity; however, a clear effect of hydrated lime was observed from the previous project using *SP2* mixes. By comparing the APA performance from the untreated *SP2* mixtures to the untreated *SP5* mixtures, the contribution of polymer-modified binder and high-quality aggregates to the rutting-related moisture-damage resistance was verified.
- The two local-scale tests demonstrated identical results. Binder PG 64-22 was much less resistant to moisture damage than binder PG 70-28, and the effect of additives was more visible with binder PG 64-22 than with PG 70-28. The effect of the binder was even more impressive when the samples were subjected to longer moisture conditioning. Even if it may not be completely conclusive at this moment, hydrated lime seems to perform slightly better than other additives, particularly with a longer conditioning time. There was no remarkable difference between two additives (fly ash and cement).
- The local-scale pull-off test results and global-scale (asphalt concrete mixture scale) test results from the AASHTO T-283 exhibited a close correlation on the tensile strength values among mixtures. This implies that the evaluation of component characteristics, such as the adhesive fracture potential between binder and aggregate, can help better identify moisture-damage mechanisms and their impacts on pavement performance. Testing of component

characteristics will be significantly beneficial, since it is much more economical and efficient than testing asphalt concrete samples.

- Numerical modeling of the pull-off testing successfully simulated the progressive degradation to complete adhesive fracture (debonding) of each different binder-additive-aggregate system with increasing moisture conditioning. Resulting model parameters, such as the *n*-value, physically identifies the rate of degradation that was sensitive to the use and types of additives. The positive effect of anti-stripping additives was demonstrated in a more scientific fundamental manner.

5.2 Recommended Further Studies

- Findings from this study should be validated with more laboratory data and field performance observations (if available).
- Based on successful accomplishments of this project, a consequential study to investigate fly ash as an alternative additive in asphalt mixtures is recommended. The effect of fly ash as a potential additive to reduce moisture damage was observed in this study, but the overall effect of fly ash on other types of distresses, such as rutting and cracking, has not yet been investigated. Due to its great economical characteristics and other engineering benefits of fly ash, research efforts investigating fly ash as a supplemental material for asphaltic pavements is considered to be a timely and necessary step.

5.3 NDOR Implementation Plan

The Nebraska Department of Roads will review field performance of similar mixes and different binder grades to substantiate the polymer binder benefits and review the potential to reduce the amount of hydrated lime in mixes that contain these highly polymer modified binders.

NDOR is interested in further research regarding the using of Class C fly ash and Portland cement.

References

AASHTO. 1986. Resistance of Compacted Bituminous Mixture to Moisture Induced Damage: ASSHTO T-283. Washington D.C.: American Association of State Highway and Transportation Officials.

Airey, G., Y. Choi, A. Collop, A. Moore, and R. Elliott. 2005. "Combined Laboratory Ageing/Moisture Sensitivity Assessment of High Modulus Base Asphalt Mixtures." *Journal of the Association of Asphalt Paving Technologists*. 74: 307-346.

Ali, N., J.S. Chan, S. Simms, R. Bushman, and A.T. Bergan. 1996. "Mechanistic Evaluation of Fly Ash Asphalt Concrete Mixtures." *Journal of Materials in Civil Engineering*. 8, no. 1: 19-25.

Aschenbrener, T. 1995. "Evaluation of Hamburg Wheel-Tracking Device to Predict Moisture Damage in Hot Mix Asphalt." *Transportation Research Record*, 1492: 193-201.

Aschenbrener, T. 2002. "Survey on Moisture Damage of Hot Mix Asphalt Pavements," Denver, Colorado: Colorado Department of Transportation.

ASTM. 2005. Standard Practice for Effect of Water on Bituminous-Coated Aggregate Using Boiling Water: ASTM D 3625. West Conshohocken, Pennsylvania: ASTM International.

ASTM. 2009. Pull-off Strength of Coatings Using Portable Adhesion Testers: ASTM D 4541. West Conshohocken, Pennsylvania: ASTM International.

Bhasin, A., and D.N. Little. 2007. "Characterization of aggregate surface energy using the universal sorption device." *Journal of Materials in Civil Engineering*, 19, no. 8: 634-641.

Birgisson, B., R. Roque, R., G.C. Page. 2003. "Ultrasonic Purse Wave Velocity Test for Monitoring Changes on Hot-Mix-Asphalt Mixture Integrity from Exposure to Moisture." *Transportation Research Record*, 1832: 173-181.

Cheng, D., D.N. Little, R.L. Lytton, and J.C. Holste. 2003. "Moisture Damage Evaluation of Asphalt Mixture by Considering Both Moisture Diffusion and Repeated Load Conditions." *Transportation Research Record*, 1832: 42-58.

Cho, D. W. and H. U. Bahia. 2007. "Effects of Aggregates' Surface and Water on Rheology of Asphalt Films". *Transportation Research Board*, 1998: 10-17.

Copeland, A. R. 2007. "Influence of Moisture on Bond Strength of Asphalt-Aggregate System". PhD diss., Vanderbilt University.

Dassault Systèmes. 2008. ABAQUS-CAE User's Manual: Version 6.8. Pawtucket, Rhode Ireland: Hibbitt, Karlsson & Sorenson, Inc.

Dougan, C. 1991. Past and Current Use of Recycling Materials by the Connecticut Department of Transportation; Report No.343-26-91-1, Wethersfield, Connecticut: Connecticut Department of Transportation.

Epps, J. A., P.E. Sebaaly, J. Penaranda, M.R. Maher, M.B. McCann, and A.J. Hand. 2000. Compatibility of a Test for Moisture-Induced Damage with Superpave Volumetric Mix Design; NCHRP Report 444, Washington, D.C.: Transportation Research Board - National Research Council.

Fwa, T.F. and B.K. Ong. 1994. "Effect of Moisture in Aggregates on Performance of Asphalt." *Transportation Research Record,* 1454: 28-35.

Hao, P. and H. Liu, H. 2006. "A Laboratory Study of the Effectiveness of Various Additives on Moisture Susceptibility of Asphalt Mixtures". *Journal of Testing and Evaluation*, 34, no. 4.

Henning, N.E. 1974. Evaluation of Lignite Fly Ash as a Mineral Filler in Asphaltic Concrete: Report No. (2)-73. St. Paul, Minneapolis: Twin City Testing and Engineering Laboratory.

Hicks, R. G. 1991. Moisture Damage in Asphalt Concrete: NCHRP Synthesis of Highway Practices No. 175. Washington, D.C.: Transportation Research Board - National Research Council.

Hua, Y., A.D. Crocombre, M.A. Wahab, and I.A. Ashcroft. 2006. "Modelling Environmental Degradation in EA9321-Bonded Joints Using a Progressive Damage Failure Model." *Journal of Adhesion*, 82: 135-160.

Huang, S., R.E. Robertson, J.F. Branthaver, and J.C. Petersen. 2005. "Impact of Lime Modification of Asphalt and Freeze-Thaw Cycling on the Asphalt-Aggregate Interaction and Moisture Resistance Damage." *Journal of Materials in Civil Engineering*, 17, no. 6: 711-718.

Kandhal, P.S., P.S. Foo, and R.B. Mallick. 1998. A Critical Review of VMA Requirements in Superpave: NCAT Report No. 98-1, Tuscaloosa, Alabama: National Center for Asphalt Technology.

Kanitpong, K. and H.U. Bahia. 2003. "Role of Adhesion and Thin Film Tackiness of Asphalt Binders in Moisture Damage of HMA". *Journal of the Association of Asphalt Paving Technologists*, 72: 502-528.

Kanitpong, K. and H.U. Bahia. 2005. "Relating Adhesion and Cohesion of Asphalts to the Effect of Moisture on Laboratory Performance of Asphalt Mixtures". *Transportation Research Record,* 1901: 33-43.

Kassem, E., E. Masad, R. Bulut, and R.L. Lytton. 2006. "Measurements of Moisture Suction and Diffusion Coefficient in Hot-Mix Asphalt and Their Relationships to Moisture Damage." *Transportation Research Record,* 1970: 45-54.

Kennedy, T. W. and W.V. Ping. 1991. "Evaluation of Effectiveness of Antistripping Additives in Protecting Asphalt Mixtures from Moisture Damage." *Journal of the Association of Asphalt Paving Technologists*, 60: 230-263.

Kim, Y., D.N. Little, and R.L. Lytton. 2004. "Effect of Moisture Damage on Material Properties and Fatigue Resistance of Asphalt Mixtures." *Transportation Research Record*, 1832: 48-54.

Kim, Y. and J.S.E. Lutif. 2006. Material Selection and Design Consideration for Moisture Damage of Asphalt Pavement: Final Research Report No. P564. Lincoln, Nebraska: Nebraska Department of Roads.

Kim, Y., J.S. Lutif, A. Bhasin, and D.N. Little. 2008. "Evaluation of Moisture Damage Mechanisms and Effects of Hydrated Lime in Asphalt Mixtures through Measurements of Mixture Component Properties and Performance Testing." *Journal of Materials in Civil Engineering*, 20, no. 10: 659-667.

Kringos, N., A. Scarpas and A. Bondt. 2008. "Determination of Moisture Susceptibility of Mastic-Stone Bond Strength and Comparison to Thermodynamical Properties". *Journal of the Association of Asphalt Paving Technologists*, 77: 435-478.

Kringos, N., A. Scarpas and C. Kasbergen. 2007. "Three-Dimensional Elasto-Visco-Plastic Finite Element Model for Combined Physical–Mechanical Moisture Induced Damage in Asphaltic Mixes", *Journal of the Association of Asphalt Paving Technologists*, 76.

Kringos, N., and A. Scarpas. 2008. "Physical and Mechanical Moisture Susceptibility of Asphalt Mixtures". *International Journal of Solids and Structures*, Vol. 45, pp. 2671-2685.

Liljedahl, C.D.M., A.D. Crocombe, M.A. Wahab and I.A. Ashcroft. 2006. "Modeling the Environmental Degradation of the Interface in Adhesively Bonded Joints Using a Cohesive Zone Approach." *Journal of Adhesion*, 82: 1061-1089.

Little, D. N. and J.A. Epps. 2001. The Benefits of Hydrated Lime in Hot Mix Asphalt. Arlington, Virginia: National Lime Association.

Loh, W. K., A.D. Crocombe, M.M. Abdel Wahab, and A.I.A. 2003. "Modeling Interfacial Degradation Using Interfacial Rupture Elements." *Journal of Adhesion*, 79: 1135-1160.

Lottman, R. P. 1978. Predicting Moisture-Induced Damage to Asphaltic Concrete: NCHRP Report 192. Washington, D.C.: Transportation Research Board - National Research Council.

Lytton, R.L., A.E. Masad, C. Zollinger, R. Bulut, D.N. and Little, 2005. Measurements of Surface Energy and its Relationship with Moisture Damage: Technical Report No. FHWA/TX-05/0-4524-2. College Station, Texas: Texas Transportation Institute.

McCann, M. and P.E. Sebaaly. 2003. "Evaluation of Moisture Sensitivity and Performance of Lime in Hot-Mix Asphalt." *Transportation Research Record,* 1832: 09-16.

Mohamed, E. H. 1993. "Debonding Location in Asphalt Concrete Associated with Moisture Damage." *Journal of Materials in Civil Engineering*, 5, no. 4: 497-509.

Oruc, S., F. Celik and M.V. Akpinar. 2007. "Effect of Cement on Emulsified Asphalt Mixtures." *Journal of Materials Engineering and Performance*, 16: 578-583.

Parker, F. Jr. and M.S. Wilson. 1986. "Evaluation of Boiling and Stress Pedestal Tests for Assessing Stripping Potential of Alabama Asphalt Concrete Mixtures." *Transportation Research Record*, 1096: 90-100.

Ping, W. V. 1993. "Lime Treatment of Asphalt Mixtures in Improving Resistance to Moisture." *Proc., Airport Pavement Innovations, Theory to Practice.* Vicksburg, Mississippi.

Roster, J.C., J.G. Chehovits, and G.R. Morris. 1982. "Fly Ash as a Mineral Filler and Antistrip Agent for Asphalt Concrete." *Proc., Challenge of Change - 6th International Ash Utilization Symposium,* U.S. Dept. of Energy, Morgantown, West Virginia.

Solaimanian, M., D. Fedor, R. Bonaquist, A. Soltani and V. Tandon. 2006. "Simple Performance Test for Moisture Damage Prediction in Asphalt Concrete." *Journal of the Association of Asphalt Paving Technologists*, 75: 345-380.

Solamanian, M., J. Harvey, M. Tahmoressi, and V. Tandon. 2003. "Test Method to Predict Moisture Sensitivity of Hot-Mix Asphalt Pavements." In *Moisture Sensitivity of Asphalt Pavements: A National Seminar*, San Diego, California

Terrel, R. L., S. AL-Swailmi. 1994. Water Sensitivity of Asphalt-Aggregate Mixes: Test Selection. Washington, D. C.: Strategic Highway Research Program, SHRP-A-403, National Research Council.

Tunnicliff, D. G., and R. Root. 1982. "Antistripping Additives in Asphalt Concrete: State-of-the-Art." *Proc., Association of Asphalt Paving Technologists*, St. Paul, Minnesota.

Witczak, M. W., K. Kaloush, T. Pellinen, M. El-Basyouny and H. Von Quintus. 2002. "Simple Performance Test for Superpave Mix Design: NCHRP Report No. 465. Washington D.C.: Transportation Research Board, National Research Council.

Youtcheff, J. and V. Aurilio. 1997. "Moisture Sensitivity of Asphalt Binders: Evaluation and Modeling of the Pneumatic Adhesion Test Results". *Proc., 42th Annual Conference of Canadian Technical Asphalt Association,* Ottawa, Ontario, Canada.